SEMMELWEIS EGYETEM

DOKTORI ISKOLA

Ph.D. értekezések

3013.

MAJER ALIZ

A vérkeringési rendszer normális és kóros működésének mechanizmusai
című program

Programvezető: Dr. Benyó Zoltán, egyetemi tanár

Témavezető: Dr. Ruisanchez Éva, egyetemi adjunktus

Társtémavezető: Dr. Hornyák István, tudományos munkatárs

The Development of Blood-derived and Lysophosphatidic Acid Containing Scaffolds for Bone Regenerative Applications

PhD thesis

Aliz Majer PharmD

Doctoral School of Theoretical and Translational Medicine

Semmelweis University

Supervisors: Éva Ruisanchez, MD, Ph.D.
István Hornyák, Ph.D.

Official reviewers: Tímea Feller, PharmD, Ph.D.
Krisztina Ella, Ph.D.

Head of the Complex Examination Committee: István Karádi, MD, D.Sc.

Members of the Complex Examination Committee: Henriette Farkas, D.Sc.
Charaf Hassan, D.Sc.

Budapest

2024

Table of Contents

List of Abbreviations

ALP: alkaline phosphatase

ANOVA: analysis of variance

DBM: demineralized bone matrix

FBS: fetal bovine serum

FFA: free of fatty acid

FFP: fresh frozen plasma

FTIR: Fourier-transform infrared spectroscopy

GPCRs: G protein-coupled receptors

hBM-dMSCs: human bone marrow-derived mesenchymal stem cells

HSA: human serum albumin

LPA: lysophosphatidic acid

LPC: lysophosphatidylcholine

LPL: lysophospholipid

PBS: phosphate-buffered saline

PLA: phospholipase A-like enzyme

PRF: platelet rich fibrin

RM: Regenerative Medicine

TE: Tissue Engineering

TERM: Tissue Engineering and Regenerative Medicine

XTT: Cell Proliferation Kit II

1. Introduction

The two main objective of our research is to create a tissue product or medical device that can efficiently facilitate bone regeneration or help in soft-tissue regeneration. Throughout the development process, we examined two different types of implants: injectable membranes containing fibrin and freeze-dried demineralized bone matrices (DBM) coated with lysophosphatidic acid, alone or bound to human serum albumin. To achieve this goal, we must meet various criteria from diverse perspectives outlined predominantly in the relevant quality management-associated standards (1). One of these requirements is that only those types of constituents are utilized that were already evaluated and found to be safe for human application (2). This is essentially based on using materials that were found to be biocompatible and non-toxic. The degradation products of the implanted scaffold must be also well-known and non-hazardous, and both the biological and mechanical properties need to be able to mimic the damaged tissue parts closely. Most importantly, the scaffolds need to ensure the survival of cells, and preferably, the cells can proliferate and migrate to the inner structure of the matrix to allow differentiation and remodeling in the long-term (3).

In specific pathophysiological conditions, such as osteoporosis, large bone defects, or certain fractures, the natural healing process of the bone might be compromised. In these conditions, the gap between the bone fragments needs to be filled for proper bone healing. Scaffolds are materials that are engineered to contribute to the formation of new functional tissues. Bone scaffolds are good candidates for filling the gap between the damaged fragments and promoting bone healing. However, creating a cost-effective soft tissue implant sufficient for bone regeneration remains a developmental challenge (4, 5).

In the case of soft tissue deficiencies, that encompass skin-, adipogenic-, tendon-, or muscle-related tissues, a soft-tissue scaffold with lower mechanical integrity is required compared to bone replacements. These are rather embodiments that promote the natural regeneration of the tissue.

1.1. Bone regeneration

Bones are part of the skeletal system and are responsible for mechanical (providing shape, protection, integrity, and movement), synthetic (blood cell synthesis), and

metabolic (mineral storage, phosphate and calcium regulation, fat storage, and role in acid-base balance) functions of the body.

The primary constituents of bone tissue can be classified as cellular and non-cellular elements. The cellular components of bone tissue comprise osteoblasts, osteocytes, osteoclasts, and osteogenic precursor cells (mesenchymal stem cells, MSCs). The cellular elements of bone are responsible for the synthesis, regulation, deposition, and mineralization of bone matrix (6). The non-cellular component of the bone contains approximately 30% organic and 70% inorganic substances (7). The organic phase mainly comprises collagen and a few non-collagenous proteins, while the inorganic phase incorporates mineral salts.

Bone healing is a complex and well-coordinated event. The three main phases of the bone healing process are inflammation, bone development and bone remodeling (8). Following fracture or trauma, an immediate inflammatory response occurs, and an initial hematoma containing red blood cells, platelets and fibrin is produced. Pro-inflammatory factors, such as interleukin-1 and interleukin-6, tumour necrosis factor-alpha, macrophage colony-stimulating factor, and inducible nitric oxide synthase are secreted. Bone marrow macrophages modulate the crosstalk between osteoclasts and osteoblasts, and they also secrete growth factors and chemokines that are essential for the migration of MSCs to the site of the injury. MSCs are also vital in bone healing as they are multipotent and can differentiate into many cell types (9, 10). Bone production is initiated when the blood clot formed by inflammation is substituted with fibrous tissue and cartilage. During remodeling, the mineralization of the soft callus occurs; thereafter, the mineralized callus is replaced with mineralized bone, and the bone gains back its original shape, size, and strength (7). The phases and the cellular and molecular events of bone regeneration are presented in Figure 1 below.

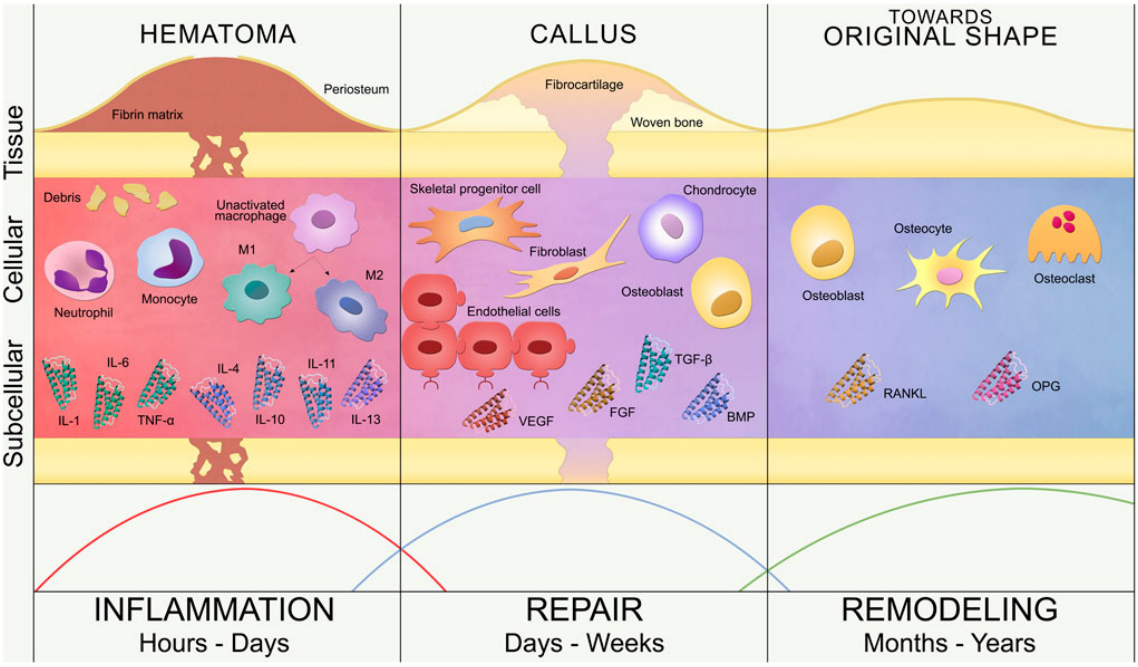

Figure 1. *Bone fracture healing process (8).* The three main phases of bone healing are inflammation, bone repair, and bone remodeling. Inflammation involves an immediate response with hematoma formation and pro-inflammatory factor secretion. During repair, skeletal progenitor cells differentiate into chondrocytes and osteoblasts, forming cartilage and woven bone, while remodeling restores the bone's original shape, size, and strength through mineralization.

Bone fracture is one of the most common traumatic problems that requires medical intervention. Fractures, especially in older people, are mainly due to osteoporosis, affecting bone tissue's regenerative potential. With aging, the proliferative and functional capabilities of macrophages and MSCs are decreased. The modulation of these cellular events might optimize the bone healing process (10, 11). Bone grafts can promote bone formation by stimulating the migration of MSCs and the ingrowth of host blood vessels into the matrix. Bone grafts can derive from auto-, allo-, or xenogeneic sources. The treatment of bone loss - as a result of trauma, osteomyelitis, tumour surgery, or osteolysis - is also a challenging problem in the orthopaedic field. The most frequently used treatment is to fill the defective sites with bone implants of either auto- or allogeneic origin (12).

1.2. Tissue engineering and regenerative medicine

Within the human body, there are tissues with limited or lacking regeneration capability. The main objective of Tissue Engineering and Regenerative Medicine (TERM) is to replace and repair lost or damaged tissues by stimulating the natural regeneration process. TERM is a multidisciplinary field that merges basic sciences, such as nanotechnology, material science, biomechanics, cell biology, and medical sciences, to promote *in vivo* tissue or organ regeneration (13).

In particular, tissue engineering (TE) aims to fabricate three-dimensional (3D) scaffolds that can be used to reconstruct and regenerate damaged tissues. In TE, scaffolds are typically seeded with the use of cells or are supplemented with growth factors. Then they are either cultured *in vitro* for tissue generation, which can be later implanted, or directly embedded into the injured site, where the regeneration is induced *in vivo* (3). Scaffolds provide the embodiment or structural support for cell and tissue growth and differentiation. Cells act as the biological trigger that stimulates endogenous regeneration. They attach to the scaffolds' surface; thus, the scaffold can be implanted *in vivo.* Growth factors also play an essential role during development and tissue healing by inducing proliferation, migration, differentiation, multicellular morphogenesis, and vascularization (14).

On the other hand, regenerative medicine (RM) uses different strategies, including cell-based therapy, gene therapy, and immunomodulation, to enhance regeneration (15). Cell-based therapies stimulate endogenous repair through extracellular factors, extracellular vesicles, or differentiation and functional replacement of endogenous cell types (16). Stem cells have been used routinely to repair injured tissues or organs for decades. Mesenchymal stem cells are multi-lineage cells, capable of self-renewal and differentiation into various cell types (17), which play vital roles in tissue healing and regenerative medicine. Bone-marrow-derived MSCs (BM-dMSCs) are the most frequently used stem cells in cell therapy and tissue engineering (18). The localization of MSCs to the injury site is a crucial step during tissue healing to avoid unintended differentiation and potential overpopulation (10). The localization of MSCs is also challenging as the local environment in a living system can permanently affect the differentiation, which cannot be kept under Control, compared to an *in vitro* system that

consists of reduced variables. Thus, to have a precise intended use and limited variables, we preferred the approach where the cellular components are reduced or completely removed from the development, and the living system's regenerative capability is utilised with a suitable scaffold that enhances the healing process.

1.2.1. Requirements of scaffold development

Scaffolds are implants that provide the appropriate environment for the regeneration of tissues and organs. Regardless of the tissue type, there are some general criteria that the designed scaffold should meet. First, it must be biocompatible: the attachment, normal function, migration, and proliferation of the cells are necessary for proper implantation. Second, it must be biodegradable to allow the cells to produce their own extracellular matrix. The products of biodegradation should also be non-toxic. Third, the scaffold should have mechanical properties similar to the host tissue. Fourth, the architecture of a scaffold also plays an important role during scaffold construction to regain the body part's original function. Suppose the scaffold is not intended to be inert, and cellular attachment, migration, and differentiation must occur during regeneration. It should have a porous structure to facilitate host tissue integration upon implantation: vascularization, new tissue formation, and remodeling.

Last but not least, the manufacturing technology should be cost-effective and translatable to the clinic (3, 19). From the regulatory point of view, it also needs to be kept in mind that the envisioned product eventually needs to fall into one of the tissue product, medical device or pharmaceutical product categories. Among these categories, a tissue product requires a relatively reduced amount of regulatory, quality management and administrative tasks; thus, we aimed to develop a scaffold that can be regulated as a tissue product.

Based on the type of materials used, scaffolds can be classified as natural biological scaffold materials, synthetic biodegradable polymer scaffold materials, composite scaffold materials, and nano-scaffold materials (20). The use of decellularized matrices as scaffolds has become widespread due to the limitations of synthetic scaffolds, such as the lack of biocompatibility, possible immune response, infection, extrusion, wear, and degradation (21, 22). Different biomaterials and processing technologies can be considered for optimal scaffold development depending on the TERM strategy. The most

promising and widely used scaffold processing technologies are solvent casting with particulate leaching (23), freeze-drying (24), gas foaming (25), fibre bonding and electrospinning (26), phase separation (27), and 3D printing methodologies (28).

1.2.2. Soft tissue implants

Soft tissue includes a variety of tissues, such as skin, tendon, muscle, cartilage, nerves, fascia, intervertebral disc or blood vessels. Soft tissue implants can be defined as materials that mimic the original function of a non-weight-bearing tissue or body part and are generally used to reconstruct tissue defects due to congenital defects, disease, trauma, and ageing. Nowadays, various biomaterials (materials engineered to interact with biological systems for medical purposes) are investigated for soft tissue regeneration, including ceramics, bio-glasses, polymers, and hydrogels (29).

Biopolymers can be applied as soft tissue implants. Due to their similarities to the extracellular matrix, biodegradability, easy utilization, and good biological properties, they are often used in TE. Polymeric membranes can be produced by using natural polymers, such as polysaccharides (e.g., chitosan, cellulose, alginate) or proteins (e.g., silk fibroin, collagen, elastin) (30).

The concept of guided bone regeneration uses barrier membranes to treat large bone defects. In large bone defects, bone regeneration is required in large quantities and might be beyond the potential self-healing. In that case, the membrane acts as a barrier to prevent soft tissue invasion into the defect, guiding bone regeneration. Furthermore, these membranes also show osteoinductive, osteogenic, and angiogenic properties. Regarding bone regeneration, their use is mainly advantageous in sites with limited mechanical loading, such as in cranial and maxillofacial applications (31). Collagen membranes are widely investigated for regenerative applications due to their excellent tissue integration, fast vascularization, and ability to promote wound healing. On the other hand, their inferior mechanical strength and rapid biodegradation are disadvantageous during utilization. However, these properties can be improved using chemical, physical, and biological cross-linking methods. Furthermore, the addition of active molecules, e.g., platelet-rich fibrin and peptides, positively influences osteogenic differentiation (30).

Demineralized bone matrices (DBM) belong to the family of decellularized scaffolds and are further processed by acidic extraction. The allogeneic bone loses its mineralized

components through this procedure, while the collagen, non-collageneous proteins, and growth factors (e.g., bone morphogenic proteins, BMP) remain intact. Due to its BMP content, osteoinductive and osteoconductive (the ability of a bone substitute material to encourage bone growth onto its surface) properties, DBM can be used efficiently as a bone-graft substitute or extender to initiate a more rapid and predictable bone regeneration process (32). After decalcification, BMP can be released from the surrounding mineral components and exert its osteoinductive potential. The remaining collagen proteins provide a 3D structure favouring vascular and cellular ingrowth (33). Fresh-frozen, freeze-dried, or demineralized bone are commonly used in regenerative medicine as bone replacement interventions (12). The freeze-drying technique allows the required disinfection of DBM with chemicals since these agents are eliminated from the allograft during freeze-drying. However, this procedure lowers the scaffold's osteoinductive and osteogenic capability, resulting in unreliable incorporation (34). According to previous studies, serum albumin-coated bone allograft (BoneAlbumin) can facilitate new bone formation in non-union and critical size defect models in rats (34-37). Furthermore, serum albumin coating improves the biocompatibility of freeze-dried bone matrix. Human serum albumin (HSA) can enhance the adherence and proliferation of BM-dMSCs on bone allografts (34).

Furthermore, the mentioned biomaterials are also suitable for *in situ* delivery of various pharmaceutical compounds. Local drug delivery might enhance effectiveness and safety compared to systematic drug administration (29).

1.3. Fibrinogen and fibrin

Fibrinogen is a 340-kDa homodimeric glycoprotein consisting of six polypeptide chains. Under physiological conditions, fibrinogen is present in high plasma concentrations (2-5 mg/mL). However, plasma fibrinogen levels can increase to 7 mg/ml during acute inflammation. Fibrinogen is primarily synthesized in hepatocytes and converted into insoluble fibrin, mediated by thrombin, during coagulation. Thrombin cleaves the fibrinopeptides Aα and Bβ off from fibrinogen, forming fibrin monomers. These monomers are polymerized into fibrin protofibrils, creating a structural fibrin network within the clot (Figure 2). The thrombin concentration is crucial during fibrin formation. High thrombin concentrations produce clots resistant to fibrinolysis and thus

can cause thrombosis. Low concentrations of thrombin result in the formation of highly fibrinolysis-sensitive clots, which might lead to bleeding. Fibrin and fibrinogen are key in homeostasis, angiogenesis, inflammation, wound healing, and other physiological and pathophysiological processes (38, 39).

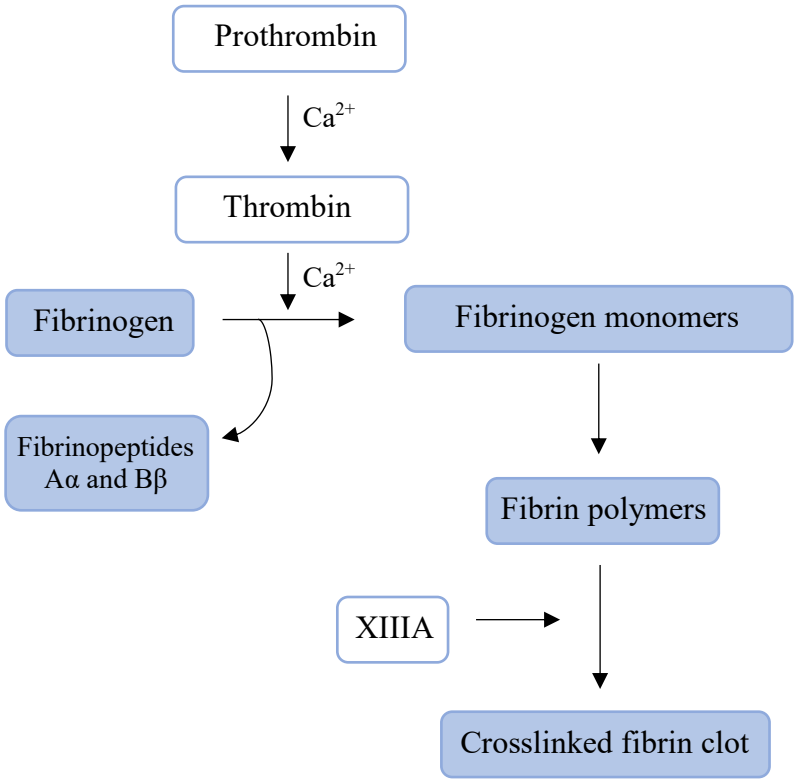

Figure 2. *The role of fibrinogen in blood clotting. Figure adapted from John MJ et al. (39).* Fibrinogen, synthesized in hepatocytes, is converted into insoluble fibrin by thrombin during coagulation. Thrombin cleaves fibrinopeptides Aα and Bβ from fibrinogen, forming fibrin monomers that polymerize into fibrin protofibrils, creating a structural network within the clot.

1.3.1. The application of fibrin in regenerative medicine

The preparation of fibrin can be achieved through various pathways. However, fibrin is prepared with the natural polymerization process from fibrinogen. The initial fibrinogen content can be purified to contain over 90 % per cent, e.g., in the pharmaceutical preparation called fibryga®, which is intended to supplement fibrinogen intravenously (40). Another product is an *in situ* fibrin-forming application called a duploject system, which contains linked syringes that mimic the blood clotting by

simultaneously mixing fibrinogen and thrombin with sufficient calcium chloride solution. The intended use of this medical device is to form a sealant to close surgical wounds (41).

Fibrin is widely used in regenerative medicine, for instance, as a delivery system (42), as an adhesive during surgeries (43), in wound healing (44), or for bone repair (45). Due to its biocompatibility, controllable biodegradability, cell attachment-promoting properties, and growth factor content, it is also suitable for tissue engineering as a three-dimensional scaffold (46). It is possible to prepare fibrin from whole blood, which does not involve the addition of anticoagulants. However, the procedure must be done relatively quickly in this case. Whole blood needs to be centrifuged immediately after blood drawing in a serum tube to allow the formation of platelet-rich fibrin (PRF), which can be further centrifuged to acquire a fibrin membrane that does not contain anticoagulants (47). With this procedure, blood coagulation is already activated during the process. To avoid activation, plasma can be used and activated separately to allow fibrin formation. With the use of plasma, we can postpone activation and achieve a concentrated initial fibrinogen concentration as well. This procedure involves either cryoprecipitation or chemical precipitation with ethanol, ammonium sulfate, or polyethylene glycol. The main advantage of cryoprecipitation over the other methods is that it does not require potentially cytotoxic chemicals (45). Fibrin membranes can be isolated from fresh frozen plasma (FFP) or cryoprecipitate produced by whole blood centrifugation or plasmapheresis (48). Cryoprecipitate is a plasma-derived product rich in fibrinogen, factor VIII, factor XIII, von Willebrand factor, and fibronectin. FFP is thawed between 1 and 10°C and centrifuged during its preparation. The insoluble precipitate is then resolved in plasma and refrozen (49). Fibrin can be produced by activating the plasma, which can be achieved by adding thrombin and Ca^{2+} ions (50) or Ca-gluconate (51).

1.4. Lysophosphatidic acid

Lysophosphatidic acid (LPA) is a naturally occurring small bioactive glycerophospholipid (molecular mass: 430–480 Da) that is present in the systemic circulation in high nanomolar to low micromolar concentrations (52).

LPA can be synthesized through two major synthetic pathways. During the first pathway, precursor phospholipids (phosphatidylcholine, phosphatidylserine, or

phosphatidylethanolamine) are converted to their corresponding lysophospholipids (LPLs), such as lysophosphatidylcholine (LPC), lysophosphatidylserine (LPS) or lysophosphatidylethanolamine (LPE). In platelets, LPLs are produced by phospholipase A-like enzymes (PLA_1 or PLA_2) expressed by the cells. In plasma, LPC is produced by lecithin-cholesterol acyltransferase (LCAT) and PLA_1 activity. Then, these LPLs are converted to LPA by a lysophospholipase D plasma enzyme called autotaxin. On the other hand, LPA can be produced from phosphatidic acid directly by PLA_1 or PLA2. The degradation of LPA is mediated by lipid phosphate phosphatases (LPPs), LPA acyltransferase, and various phospholipases (53, 54).

It is crucial to emphasize that the term "LPA" does not denote a singular molecule but rather a family of molecules. Its members can be found in body fluids with different concentrations, and they activate diverse biological responses. All LPA molecules comprise a glycerol backbone connected to a phosphate head group and are typically ester-linked to an acyl chain (53). The formed LPA species' acyl chain length and degree of saturation are different (Figure 3). There are 16:0 > 18:0 > 20:4 > 18:1 > 18:2 LPAs identified in resting and activated platelets. By contrast, in plasma, the rank order is 18:2 > 18:1 ≥ 18:0 > 16:0 > 20:4, whereas in serum the order is 20:4 > 18:2 > 16:0 ≥ 18:1 > 18:0 (Table 1) (54-58).

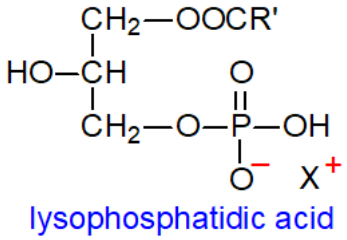

lysophosphatidic acid

(where X = H, Na, K, Ca, etc.)

R'	Names
Palmitic acid	16:0 LPA, Palmitoyl-LPA
Palmitoleic acid	16:1 LPA, Palmitoleyl-LPA
Stearic acid	18:0 LPA, Stearoyl-LPA
Oleic acid	18:1 LPA, Oleoyl-LPA
Linoleic acid	18:2 LPA, Linoleoyl-LPA
Arachidonic acid	20:4 LPA, Arachidonoyl-LPA

Figure 3. *Chemical structure of common LPA species and their numerical abbreviations. Figure based on the publication of Pagés et al. (59).* All LPA molecules have a glycerol backbone connected to a phosphate head group, typically ester-linked to an acyl chain (R'). The acyl chains of these LPA species vary in length and degree of saturation.

The numerical abbreviations refer to the length of acyl chains, and the degree of the saturation of the LPA species. These abbreviations will be used later in the thesis.

Table 1. *The concentration of different LPA species in human platelets, plasma, and serum (57, 58).*

		LPA (µM ± SD)				
		16:0	18:0	18:1	18:2	20:4
Platelets		2.17 ± 0.70	2.11 ± 0.78	0.47 ± 0.30	0.12 ± 0.39	1.06 ± 0.45
Plasma	Male	0.08 ± 0.03	0.06 ± 0.04	0.13 ± 0.05	0.27 ± 0.06	0.06 ± 0.02
	Female	0.09 ± 0.03	0.1 ± 0.06	0.11 ± 0.05	0.37 ± 0.13	0.08 ± 0.02
Serum	Male	0.09 ± 0.04	0.07 ± 0.02	0.14 ± 0.10	0.32 ± 0.08	0.22 ± 0.10
	Female	0.12 ± 0.04	0.09 ± 0.05	0.21 ± 0.22	0.50 ± 0.16	0.64 ± 0.23

Extracellular LPA acts through at least six specific G protein-coupled receptors (GPCRs), $LPAR_{1\text{-}6}$, and regulates various cellular signaling pathways (Figure 4). LPA has a crucial role in numerous biological responses, including cell adhesion, migration, proliferation (60), differentiation (61), vascular development, wound healing, apoptosis regulation, and immunity (62, 63).

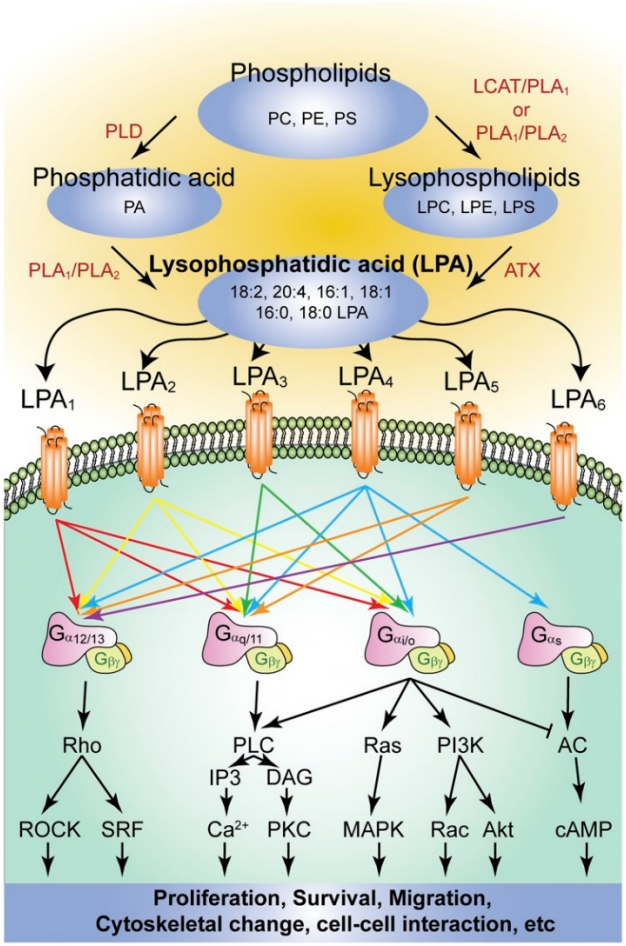

Figure 4. *The major routes of LPA synthesis and the activated signaling pathways (53).*

Similarly to long-chain fatty acids, LPA binds with high affinity to serum albumin, the main extracellular LPA binding protein, at a molar ratio of approximately 3:1 (64, 65). LPA binds to the albumin's primary high-affinity fatty acid-binding sites (64). Albumin is necessary for the biological activity of LPA, and albumin concentration is critical for activating LPA receptors in a receptor-type-specific manner (66). Intracellularly, LPA can be bound to and transported by fatty acid-binding proteins and gelsolin (64, 67).

1.4.1. The role of LPA in bone cell biology

LPA influences skeletal homeostasis and bone biology. In $LPAR_1$ knock-out (KO) mice, decreased bone density, shorter bone length, and craniofacial dysmorphism can be observed. In contrast, $LPAR_4$ KO mice show higher bone mass, trabecular number, and thickness (68, 69).

Bone cells, such as BM-dMSCs, osteoblasts, osteocytes, and osteoclasts, play significant roles in bone homeostasis and repair. Under physiological conditions, osteoblast-produced LPA is present in bone tissue, and under some pathophysiological conditions, such as fracture healing, bone cells are exposed to high levels of platelet-derived LPA (70). LPA induces various cellular effects in different bone cells, including proliferation, differentiation, survival, and migration (71).

Although there is no direct evidence that BM-dMSCs produce LPA, autotaxin - a lysophospholipase D enzyme that hydrolyses LPC into LPA - is secreted by human BM-dMSCs (hBM-dMSCs) (72). LPA receptors have been identified in different BM-dMSCs. However, in hBM-dMSCs, $LPAR_1$ was observed to be the most frequently detected LPA receptor (73). Different effects of LPA have been described in MSC biology. In addition to inducing migration (74), it was shown that LPA induces osteoblastic differentiation in hBM-dMSCs, which effect was completely absent in the case of $LPAR_1$ inhibition. At the same time, the downregulation of LPA_4 expression increased osteogenesis (60). Furthermore, Chen *et al.* proved that LPA protects hBM-dMSCs against hypoxia and serum-deprivation-induced apoptosis (75). In another study, LPA was found to rescue BM-dMSCs from hydrogen peroxide-induced apoptosis (76). These findings suggest that LPA can act as a potent survival factor for MSCs. One of the most significant difficulties of successful *in vivo* translation of cell therapies is maintaining cell survival after implantation; therefore, developing novel methods for enhancing cell survival is crucial.

It is known that osteoblasts produce LPA under physiological conditions. In different types of osteoblasts, LPA receptors are expressed at varying degrees. For instance, according to Aki's research group, human osteoblastic SaM-1, SaOS-2, HOS, and MG-63 cells express $LPA_{1,2}$ receptors. However, the expression of $LPAR_3$ was not detected in SaM-1 and SaOS-2 cells (77). LPA promotes the survival and proliferation of osteoblasts (78). Grey and colleagues showed that LPA inhibited serum deprivation-induced apoptosis dose-dependently in the SaOS-2 cell line (79). Furthermore, it was also found that LPA enhanced the growth of human osteoblasts and the activity of alkaline phosphatase, an early marker of osteogenic differentiation (80). Likewise, Mansell *et al.* established that albumin-bound LPA and calcitriol cooperate to promote osteoblast maturation on titanium and hydroxyapatite-coated surfaces (81) and improve human osteoblastogenesis (61). According to Peyruchaud's research group, osteoblast-specific

$LPAR_1$ KO mice show reduced bone mineralization, decreased cortical thickness, and increased bone porosity (82).

Osteocytes regulate the cellular activity of osteoblasts and osteoclasts. $LPA_{1,2,4}$ receptors have been identified in these cell types (83). In osteocytes, LPA induces dendrite outgrowth and motility, essential for regulating the surrounding bone cells (70).

Osteoclast differentiation and activation are crucial in bone remodeling in health and disease. Osteoclasts are formed through multiple phases, such as cell-to-cell contact, fusion, and differentiations. In bone-resorbing osteoclasts, LPA supports osteoclastogenesis via its role in osteoclast fusion (84). In addition, in osteoclasts, LPA exposure increases Ca^{2+}-mediated intracellular signaling, evokes retraction and promotes cell survival (85).

1.4.2. The potential uses of LPA in tissue engineering

Due to its abovementioned effects on different bone cells, ready availability, and relatively low cost, LPA might be a promising candidate for applications in bone regeneration (73). Furthermore, LPA contributes to angiogenesis, which is also a key step during the bone regeneration (86). Recently, some biomaterial studies have supported the potential use of LPA in bone tissue engineering applications. However, there are still some challenges with the *in vivo* application of LPA. LPA is quickly degraded *in vivo* by lipid phosphate phosphatases (87); thus, LPA requires a carrier that allows the successful delivery of the lipid. The most modern strategies for RM utilize biomaterials, such as hydrogels or polymer scaffolds, that can promote delivery to larger defects. HSA, a natural LPA transporter protein, might also be a good candidate due to its beneficial effects on hBM-dMSCs and bone regeneration (34, 35, 37).

A study reported by Bosetti *et al.* indicates that LPA and 1,25-dihydroxy vitamin D3-enriched injectable scaffold can fasten bone fragments, leading to their apposition and new bone formation (4). Furthermore, Binder *et al.* showed that physically entrapped LPA containing alginate hydrogel enhanced hBM-dMSCs survival *in viv*o (88). It has also been observed that porous scaffolds of degradable chitosan/beta-tricalcium phosphate containing LPA or LPA analogue enhance mineral deposition significantly in

osteoblasts in *in vivo* murine femoral critical size defect model. However, only LPA analogue treatment increased new bone formation compared to the control group (71).

2. Objectives

Although tissue engineering and regenerative medicine is a highly investigated, emerging field, tissue and organ repair still represents a clinical challenge. The overall aim of our research is the development of a soft tissue implant sufficient for bone regenerative application. The two types of implants we aim to test during development are injectable, fibrin-containing membranes and freeze-dried, human serum albumin-bound lysophosphatidic acid-coated demineralized bone matrices (DBM). In the experiments, we aim to investigate if these scaffolds are suitable for further *in vivo* utilization.

First of all, in our experiments, we aimed to prepare fibrin membranes from fresh frozen plasma and different concentrations of cryoprecipitate samples. The very first criterion of any scaffold for tissue engineering is that it must be biocompatible. Therefore, in our experiments, we intended to investigate if the fibrin membranes are suitable for cell attachment. Cell attachment-promoting properties of a scaffold contribute to proper implantation and thus serve as a piece of important information during the developmental process.

Furthermore, for subsequent DBM preparation, our very first objective was to develop the appropriate coating solution. Hence, we aimed to assess the complex formation between human serum albumin (HSA) and lysophosphatidic acid (LPA) in aqueous solutions.

Cell proliferation and migration are known as key steps of proper implantation and new tissue development. Thus, we aimed to determine the effect of the most abundant, albumin-bound 16:0, 18:1, and 18:2 LPA species on the proliferation and migration of human bone marrow-derived mesenchymal stem cells (hBM-dMSCs). Furthermore, we planned to evaluate the biocompatibility and cell attachment capacity of LPA- and HSA-coated DBMs *in vitro.*

3. Methods

3.1. Cell culture

Human bone marrow-derived mesenchymal stem cells (hBM-dMSCs) were purchased from ATCC (Manassas, VA, USA). The hBM-dMSCs were seeded in T75 TC-treated culture flasks and maintained at 37°C in a 5% CO2, 95% humidified air incubator in the following stem cell medium: Dulbecco's modified Eagle's medium (DMEM) containing 4.5 g/L glucose and L-glutamine (Sigma-Aldrich, St. Louis, MO, USA) supplemented with 10% fetal bovine serum (FBS; EuroClone, Pero, Italy), 1% Penicillin–streptomycin (Sigma-Aldrich, St. Louis, MO, USA), and 0.75 ng/mL basic fibroblast growth factor (Sigma-Aldrich, St. Louis, MO, USA). The culture medium was replaced three times a week. Cells with five to eight passages were used in the present study. In addition, 18:1 (oleoyl) and 18:2 (linoleoyl) LPA were purchased from Echelon Biosciences (Salt Lake City, UT, USA), and 16:0 (palmitoyl) LPA was purchased from Avanti Polar Lipids (Alabaster, AL, USA). For stock solutions, the lipids were dissolved in methanol, dried under nitrogen gas, and reconstituted in water immediately before use.

3.2. Cryoprecipitate isolation and blood component measurement

Cryoprecipitate was isolated from fresh frozen plasma (FFP; (Hungarian National Blood Transfusion Service, Budapest, Hungary). The FFP was produced using plasmapheresis, containing citrate as an anticoagulant. 50 mL plasma was thawed overnight at 3°C, and centrifuged at 3260×g for 12 min at 3°C. Different concentrations of cryoprecipitate were isolated as follows: after centrifugation, 10, 20, 30, and 40 mL of the supernatant was removed, and the centrifuged precipitate was resuspended in the remaining 40, 30, 20, or 10 mL supernatant as visible in Figure 5. The most concentrated cryoprecipitate sample was marked as C1, followed by C2, C3, and C4 with increasing dilution. Sn1, Sn2, Sn3, and Sn4 supernatants were collected from above the precipitate, while plasma was used as a control.

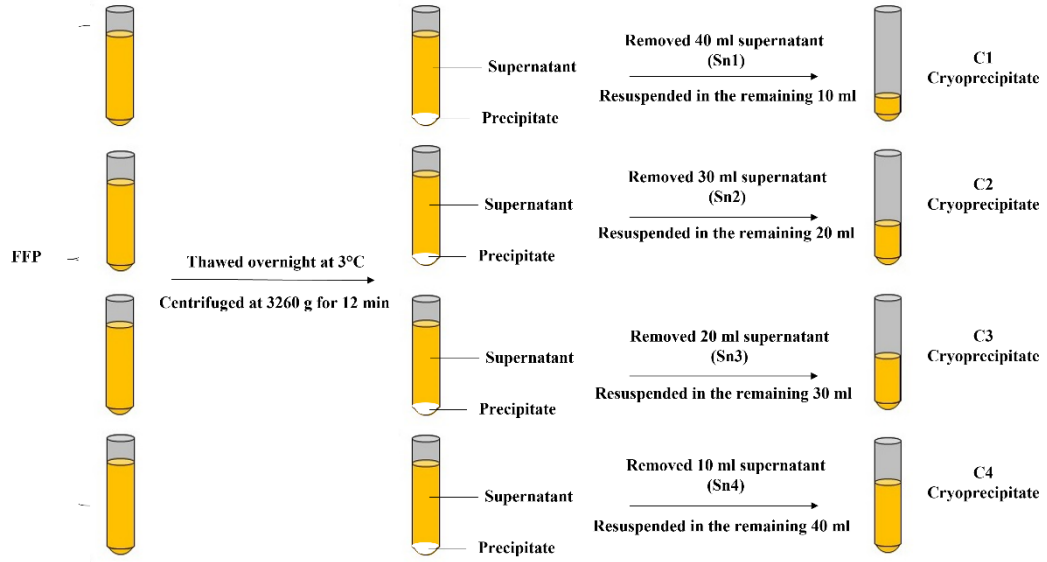

Figure 5. *Schematic demonstration of cryoprecipitate preparation from fresh frozen plasma (FFP).* 50 ml of thawed FFP (shown in yellow on the left side of the panel) was centrifuged, and a different amount of supernatant was removed subsequently. Then, the precipitate (shown in white in the middle of the panel) was resuspended in the remaining supernatant. Cryoprecipitate groups are shown on the right side of the panel, from the most concentrated (C1) to the most diluted (C4) group downwards. Figure based on the publication of Hinsenkamp et al. (89).

Fibrinogen (n = 6), haemoglobin (n = 4), albumin (n = 6), and total protein (n = 6) concentrations, and alkaline phosphatase (ALP) enzyme activity (n = 4) of control plasma and cryoprecipitate were measured using a Beckman Coulter AU5800 automated laboratory machine (Brea, CA, USA). For the quantitative determination of the platelets (n = 5), red blood cells (n = 4), and leukocytes (n = 4), Sysmex XN-1000 Sa-01 cell counter (Kobe, Japan) was used.

3.3. Fibrin membrane preparation and weight measurement

Fibrin membranes were prepared from plasma (Control), cryoprecipitate (C1, C2, C3, and C4), and pooled supernatant (Sn). The clotting was induced by adding 400 µL of 10 w/w% Ca-gluconate solution (anhydrous, Sigma-Aldrich, St. Louis, MO, USA) to 2 mL of plasma, cryoprecipitate, or supernatant on a 24-well plate. The plate was kept at 4°C for 48 h, and the fibrin clot was removed from the wall of the wells subsequently.

The clots at the bottom of the wells were centrifuged at 2020×g for 30 min at room temperature to obtain flat membranes. The membranes were freeze-dried, and their weights were measured using an analytical scale.

3.4. Assessment of albumin-LPA complex formation

Fourier-transform infrared (FTIR) spectra of HSA-bound LPA species were compared with native HSA. Infrared spectroscopy enables the identification of the characteristic stretching, vibrational and rotational changes in the molecular bonds, thus, an absorbance spectrum can be created that is unique for each molecule. The measurements were performed with a Bruker Vertex 80v (Bruker Corp., Billerica, MA, USA) spectrometer, equipped with a high-sensitivity mercury–cadmium–telluride detector, and a single reflection diamond attenuated total reflectance (ATR) accessory. We collected 128 scans at a 2 cm^{-1} resolution at the 4000–400 cm-1 spectra wavelength range. Further, 18:1, 18:2, or 16:0 LPA stock solutions of 1 mM concentration were mounted and surface-dried. A complex formation was initiated by mixing HSA and LPA with a peptide-to-lipid ratio of ~1:3 using concentrations of 300 μM and 1 mM for the HSA and the lipid, respectively. HSA- and LPA-containing solutions were mixed immediately before use.

3.5. DBM preparation

C57Bl/6 adult mice were euthanized using CO_2 inhalation. Parietal bone was identified, and cortical bone pieces were harvested with a 4 mm internal diameter trephine bur. The DBM was prepared by following the classical method originally described by Urist (90). Briefly, defatting by methanol for 24 h, washing with PBS for 5 min, followed by antigen removal by partial autolysis in 0.1 M PBS containing 10 mmol/L sodium azide and 10 mmol/L iodic acetic acid at 37°C for 48 h. Decalcination in 0.6 N hydrochloric acid at room temperature for 24 h. Washing with PBS for 5 min and whitening in 3% hydrogen peroxide at room temperature for 36 h. Washing in distilled water and then freeze drying. Thereafter, DBM pieces were soaked into stock solutions containing either PBS (Control), 18:2 LPA (100 μM), HSA (30 μM), or 18:2 LPA (100 μM) and HSA (30 μM) in combination. After 5 minutes of soaking, bone grafts were removed from the solutions, freeze-dried, and kept at -20°C until use.

3.6. Live-dead staining of hBM-dMSCs on fibrin membranes

25,000 hBM-dMSCs were seeded onto freshly isolated fibrin membranes on 24-well, ultra-low attachment plates in 2 mL of stem cell medium and cultured for six days. The culture medium was replaced every other day. Live-dead staining was performed on the seventh day to visualise the attached cells. After washing with Dulbecco's phosphate-buffered saline (PBS; Sigma-Aldrich, St. Louis, MO, USA), the membranes were stained with PBS containing 1 mM Calcein-AM (Invitrogen, Carlsbad, CA, USA), 4 mg/mL ethidium homodimer (Invitrogen), and 20 mg/mL Hoechst (Invitrogen, Carlsbad, CA, USA) for 30 min. The gels were washed for 10 min with FluoroBrite DMEM (Gibco, Paisley, Scotland), and images were taken by an inverse fluorescent Nikon Eclipse Ti2 microscope (Tokyo, Japan).

3.7. Viability of hBM-dMSCs measured by XTT

The viability and proliferation of the seeded hBM-dMSCs was measured using Cell Proliferation Kit II (XTT; Roche, Mannheim, Germany), according to the manufacturer's instructions. XTT assay is a colourimetric assay used to measure cellular metabolic activity as an indicator of cell viability, proliferation, and cytotoxicity. During the experiments, the cells were incubated with the yellow tetrazolium salt (XTT) for 4 h at 37°C, which was reduced to an orange formazan dye by the metabolically active cells. The formed formazan dye was quantified using a scanning multiwell spectrophotometer (ELISA reader). An increase in the number of viable cells increases mitochondrial dehydrogenase activity of the sample, which directly correlates with the amount of the orange formazan dye.

3.7.1. Cell attachment and proliferation on fibrin membranes

The fibrin membranes were placed into the wells of 24-well, ultra-low attachment plates in 500 µL stem cell medium, and 25,000 hBM-dMSCs were seeded on each membrane. Cell viability was measured after 24 hours of cell attachment on half of the membrane-containing wells. The rest of the membranes with the seeded cells were cultured in 2 mL stem cell medium for six additional days. The culture medium was replaced every other day. After one week, cell proliferation was examined.

3.7.2. Assessment of LPA's effect on cell proliferation

The hBM-dMSCs were seeded on 96-well plates at 10,000 cells/well in 200 µL stem cell medium and allowed to attach for 24 h. After attachment, the stem cell medium was changed to serum-free medium with or without 4% (w/v) fatty-acid-free human serum albumin (HSA, Seracare, Milford, MA, USA), and the cells were cultured in the new medium overnight. Then, the cells were treated with 18:1, 18:2, or 16:0 LPA (0.1-0.3-1-3-10 µM) for 24 h. After treatment, the cell proliferation was measured. Cell proliferation is expressed as a percentage of the data of the HSA or native control group.

3.7.3. Cell attachment capacity of coated DBMs

35,000 hBM-dMSCs were seeded on different types of DBM, placed into the wells of 98-well, ultra-low attachment plates in 200 µL of 10% fatty-acid-free FBS-containing (Sigma-Aldrich, St. Louis, MO, USA) stem cell medium. The viability of the attached cells was measured after one day of incubation. In some experiments, the cells were allowed to grow for an additional six days before measurement. Serum-free stem cell medium with or without supplementation was replaced every other day. The supplemented medium contained either 18:2 LPA (10 µM), HSA (3µM) or 18:2 LPA (10 µM) and HSA (3µM) in combination. After one week, cell proliferation was examined. Cell proliferation is expressed as a percentage of the control group's data.

3.8. Wound healing assay

The hBM-dMSCs were allowed to grow on 24-well plates in 500 µL stem cell medium until they reached a confluent monolayer. The stem cell medium was changed to serum-free medium with or without 4% HSA, and the cells were incubated overnight. A cell-free zone was created across the cell monolayer with a sterile plastic micropipette tip in each well. After washing with PBS, the cells were treated with 18:1, 18:2, or 16:0 LPA (1-3-10 µM) alone or combined with HSA. Cell migration was examined for 24 h with live cell imaging using a Nikon Eclipse Ti2 microscope. The images were analyzed after 0, 12, and 24 h of treatment, and the wound area was calculated by tracing the cell-free area in captured images using Nikon NIS-Elements Analysis Software (v.5.19, Nikon Corporation, Tokyo, Japan). The migration rate is expressed as the percentage of area reduction.

3.9. Statistical analysis

Data are presented as the arithmetic mean and standard error, and the p-values were determined by one-way analysis of variance (ANOVA), or two-way ANOVA followed by Tukey's multiple comparisons or Bonferroni posthoc test. Statistical analysis and graph plotting were performed using GraphPad Prism software (v.6.0; GraphPad Software Inc., La Jolla, CA, USA), and $p<0.05$ was considered a statistically significant difference.

4. Results

4.1. Blood components of cryoprecipitate

The number of cellular elements was measured in cryoprecipitate with different concentrations, supernatants, and control plasma. In plasma, a small number of platelets, leukocytes, and red blood cells were found in the samples. Approximately 10×10^9/L platelets were measured in the control groups. Platelets were also present in cryoprecipitate samples, and their number increased with the degree of concentration. Significant differences were found between C1 and C2, C1 and C3, C1 and C4. C1 and C2 groups showed significantly higher platelet numbers compared to the Control. Additionally, all the cryoprecipitate groups differed significantly from the Sn groups (Figure 6A). Detailed statistics of Figure 6A are shown in Table 2. More leukocytes were found in more concentrated samples; however, there was no significant difference between the measured groups. The control plasma also contained some leukocytes, but in the supernatants, their levels remained under the detectable limits (Figure 6B). The number of red blood cells was only measurable in the C1 and C2 groups (Figure 6C), while the haemoglobin level was only in the C1 group (Figure 6D); no significant differences were found between the measure groups.

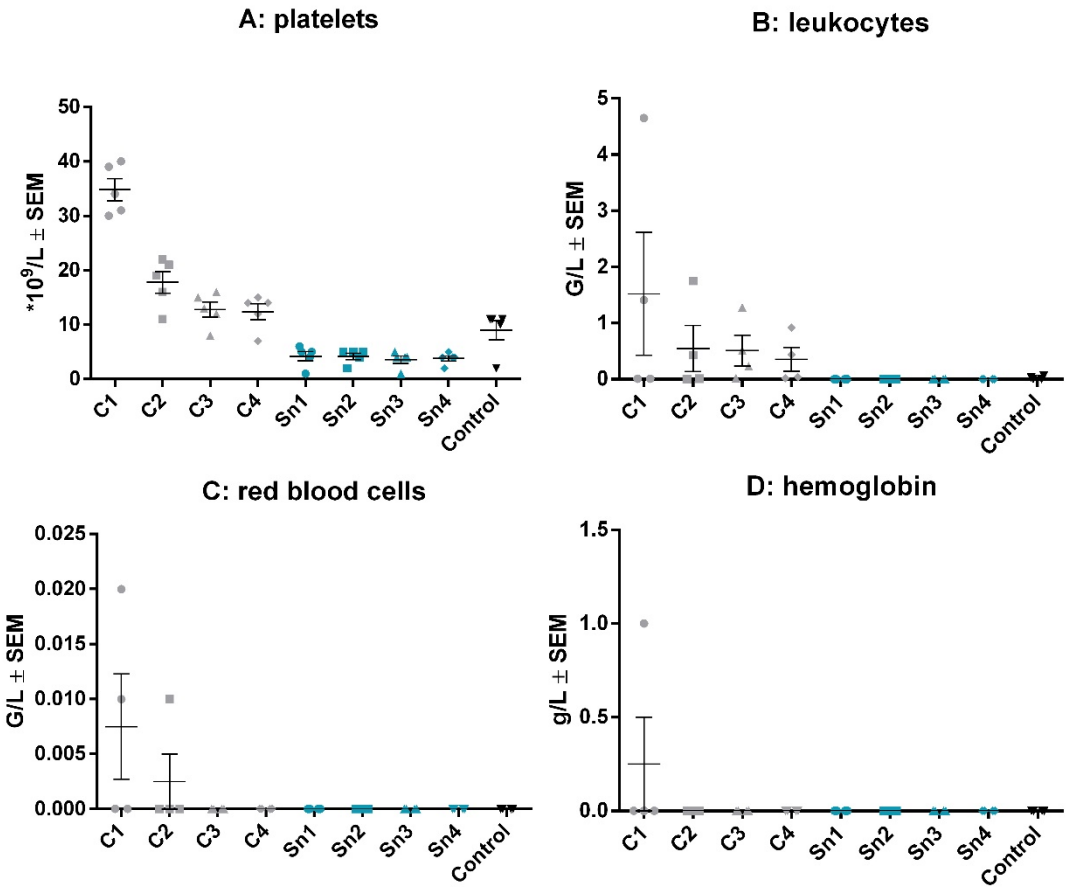

Figure 6. *Platelet (n=5)* ***(A)****, leukocyte (n=4)* ***(B)****, red blood cell (n=4)* ***(C)****, and haemoglobin (n=4)* ***(D)*** *content of different plasma-derived samples.* Data are presented as mean ± SEM (89).

Table 2. *Significant differences in platelet number between the different cryoprecipitate groups.* A one-way analysis of variance (ANOVA) with Tukey's post hoc test (89).

Significantly different groups	P values	Significantly different groups	P values
C1 - C2	< 0.0001	C2 - Sn4	< 0.0001
C1 - C3	< 0.0001	C2 - Control	0.0018
C1 - C4	< 0.0001	C3 - Sn1	0.0025
C1 - Sn1	< 0.0001	C3 - Sn2	0.0025
C1 - Sn2	< 0.0001	C3 - Sn3	0.0010
C1 - Sn3	< 0.0001	C3 - Sn4	0.0014
C1 - Sn4	< 0.0001	C4 - Sn1	0.0044
C1 - Control	< 0.0001	C4 - Sn2	0.0044
C2 - Sn1	< 0.0001	C4 - Sn3	0.0018
C2 - Sn2	< 0.0001	C4 - Sn4	0.0025
C2 - Sn3	< 0.0001		

The protein content measurements showed that cryoprecipitate with higher concentrations contained more fibrinogen. The control sample concentration was approximately 2.5 g/L, which amount was multiplied in the case of C1 (on average 6.5 g/L). C2 and C3 also showed a significant increase in the fibrinogen content compared to the control group. Furthermore, every cryoprecipitate sample had a significantly higher fibrinogen concentration than the supernatants, while the fibrinogen content of Sn1, Sn2, Sn3, and Sn4 did not differ significantly. The supernatants had significantly lower fibrinogen concentration compared to the control group (Figure 7A). The total protein concentration was also slightly affected by cryoprecipitate isolation, but only C1 and C3, C1 and C4, and C1 and the Control and supernatant groups differed significantly (Figure 7C). Albumin was detected in the samples with approximately 40 g/L concentration; however, the tendency of decreasing albumin concentration with decreasing cryoprecipitate concentration is not clear. Only the C1 group showed a significant difference compared to the supernatants. (Figure 7D). Detailed statistics of Figure 7 are shown in Table 3. ALP activity was also measurable in the examined samples, but no significant difference was observed (Figure 7B).

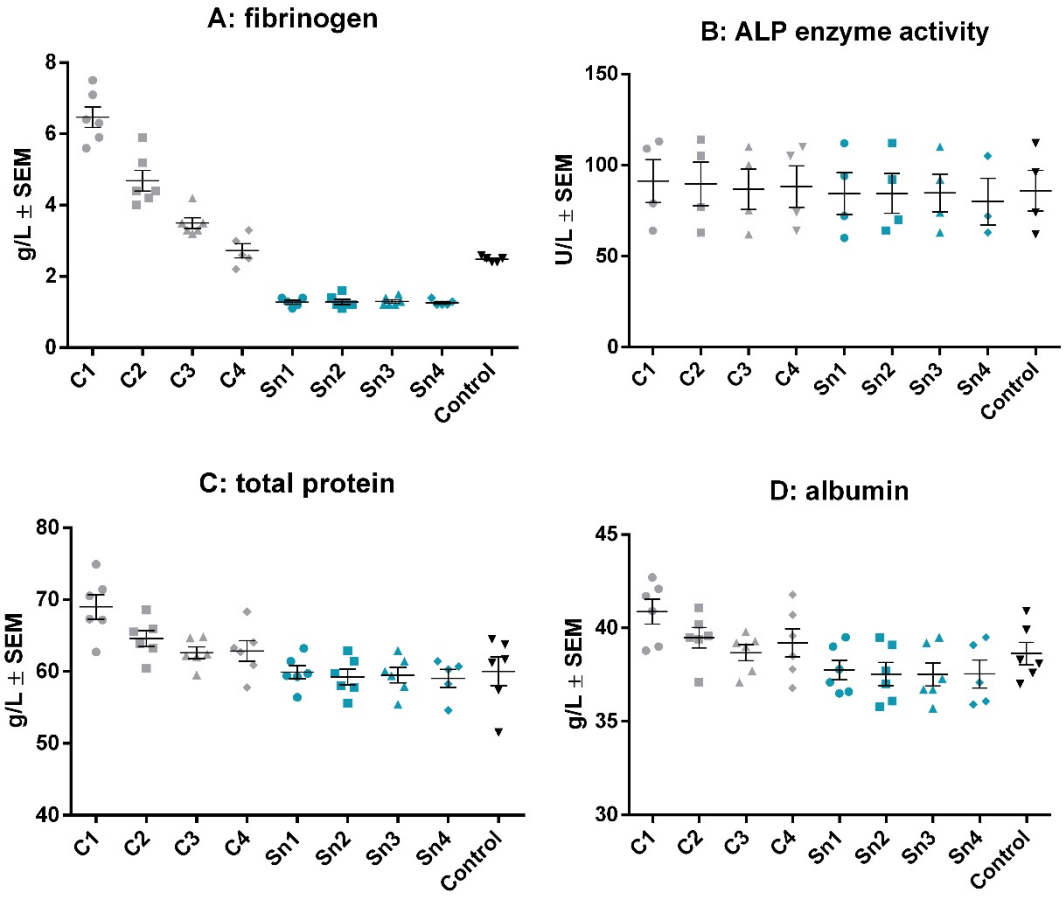

Figure 7. *Fibrinogen (n=6) (A), total protein (n=6) (C), albumin (n=6) (D) content, and ALP enzyme activity (n=4) (B) of different plasma-derived samples.* Data are presented as mean ± SEM (89).

Table 3. *Significant differences of fibrinogen, total protein, and albumin content between the different plasma-derived samples*. A one-way analysis of variance (ANOVA) with Tukey's post hoc test (89).

Significantly different groups	P values	Significantly different groups	P values
Fibrinogen		**Fibrinogen**	
C1 - C2	< 0.0001	C2 - C3	0.0004
C1 - C3	< 0.0001	C2 - C4	< 0.0001
C1 - C4	< 0.0001	C2 - Sn1	< 0.0001
C1 - Sn1	< 0.0001	C2 - Sn2	< 0.0001
C1 - Sn2	< 0.0001	C2 - Sn3	< 0.0001
C1 - Sn3	< 0.0001	C2 - Sn4	< 0.0001
C1 - Sn4	< 0.0001	C3 - Sn1	< 0.0001
C1 - Control	< 0.0001	C3 - Sn2	< 0.0001
C2 - Control	< 0.0001	C3 - Sn3	< 0.0001
C3 - Control	0.0056	C3 - Sn4	< 0.0001
Sn1 - Control	0.0012	C4 - Sn1	< 0.0001
Sn2 - Control	0.0007	C4 - Sn2	< 0.0001
Sn3 - Control	0.0008	C4 - Sn3	< 0.0001
Sn4 - Control	0.0010	C4 - Sn4	< 0.0001
Total protein		**Total protein**	
C1 - C3	0.0307	C1 - C4	0.0425
C1 - Sn1	0.0004	C1 - Sn3	0.0002
C1 - Sn2	0.0001	C1 - Sn4	0.0002
C1 - Control	0.0005		
Albumin		**Albumin**	
C1 - Sn1	0.0200	C1 - Sn3	0.0094
C1 - Sn2	0.0099	C1 - Sn4	0.0168

4.2. Weight measurements of fibrin membranes

Weight measurement of freeze-dried fibrin membranes with different thicknesses showed significant differences between C1 and C2, C1 and C3, C1 and C4, C2 and C3, C2 and C4. Every membrane isolated from cryoprecipitate samples showed significantly higher weight compared to the control group. The weight of cryoprecipitate-membranes and Control was significantly higher than membranes isolated from the supernatant. Thicker membranes showed greater weights (Figure 8). Detailed statistics of Figure 8 are shown in Table 4.

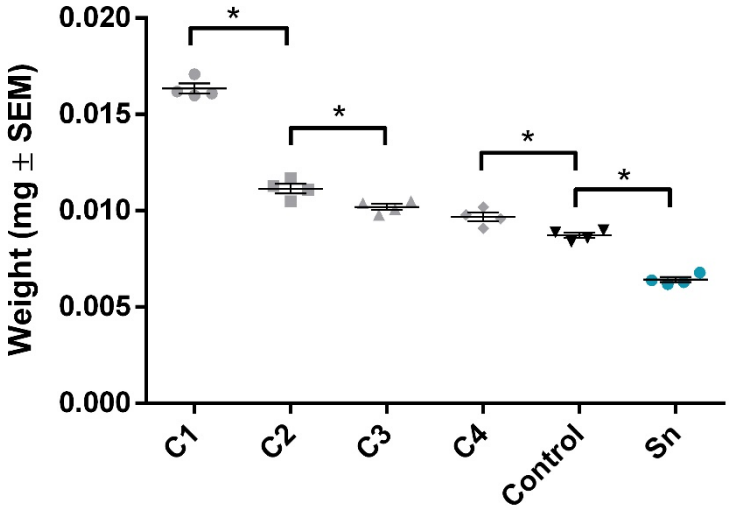

Figure 8. *Weights of freeze-dried fibrin membranes* (*p<0.05, n=4 in each group). One-way analysis of variance (ANOVA) with Tukey's post hoc test. Data are presented as mean ± SEM (89).

Table 4. *Significant weight differences between freeze-dried fibrin membranes.* (n=4 in each group). A one-way analysis of variance (ANOVA) with Tukey's post hoc test (89).

Significantly different groups	P values	Significantly different groups	P values
C1 - C2	< 0.0001	C2 - C3	0.0349
C1 - C3	< 0.0001	C2 - C4	0.0007
C1 - C4	< 0.0001	C1 - Control	< 0.0001
C1 - Sn	< 0.0001	C2 - Control	< 0.0001
C2 - Sn	< 0.0001	C3 - Control	0.0007
C3 - Sn	< 0.0001	C4 - Control	0.0349
C4 - Sn	< 0.0001	Sn - Control	< 0.0001

4.3. Live-dead staining of hBM-dMSCs cultured on the fibrin membranes

The attachment of hBM-dMSCs was analyzed by visualising live and dead cells on the surface of fibrin membranes with various thicknesses. A representative large-scale image was taken to have an overview of the hBM-dMSCs attached to the fibrin membrane (Figure 9). In addition, images were taken at 4× (Figure 10A-C and G-I) and 10× (Figure 10D-E and J-L) magnification. Live cells are stained with green, dead cells are yellow, and nuclei are blue. Only a minimal number of dead cells could be observed in the images. The cell distribution on the membranes' surfaces was not homogenous; preferred regions

with more cells can be seen in the images. Based on the microscopic images, the fibrin membrane thickness does not influence the scaffold's cell attachment capacity.

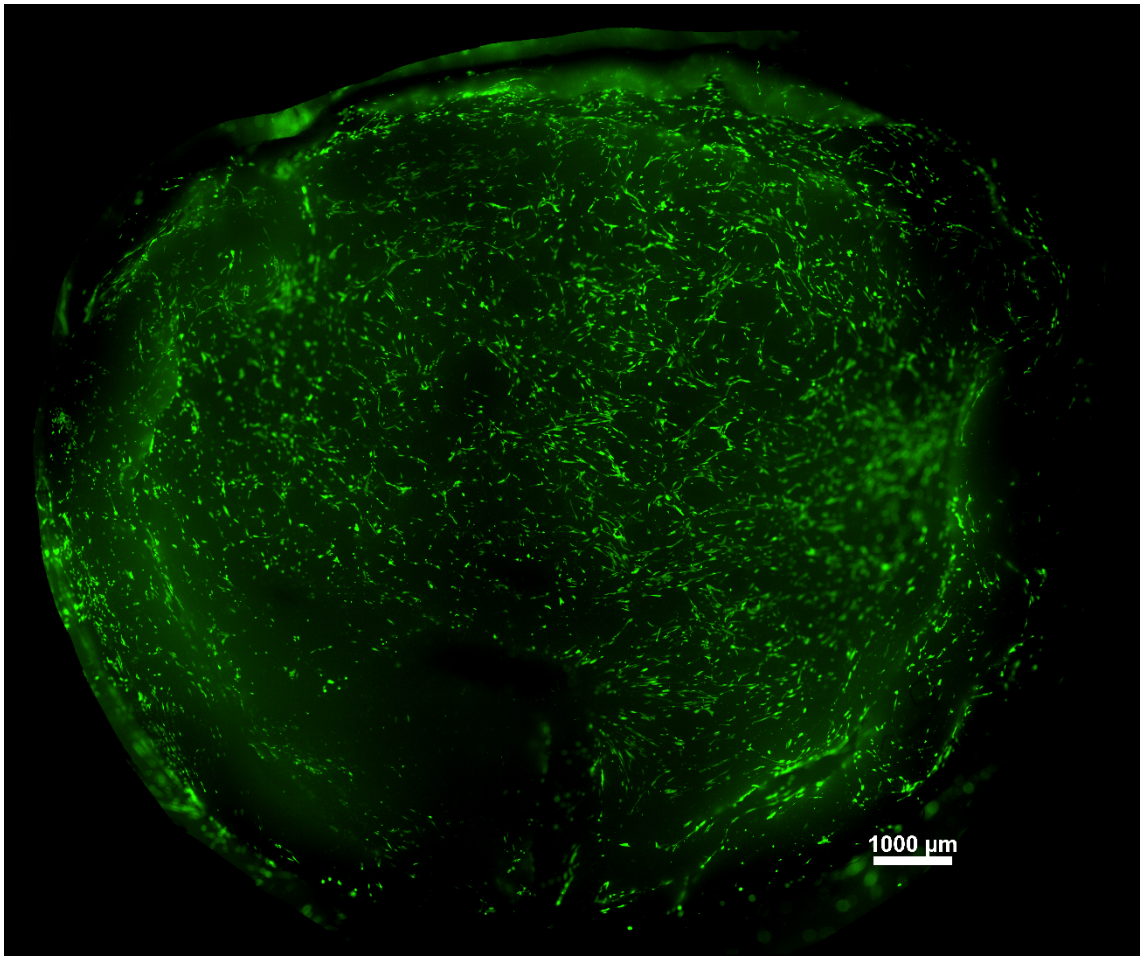

Figure 9. *Large-scale image of stained hBM-dMSCs attached to a fibrin membrane.* Live cells are shown in green, dead cells are yellow, and nuclei are blue. The scale bar represents 1000 µm (89).

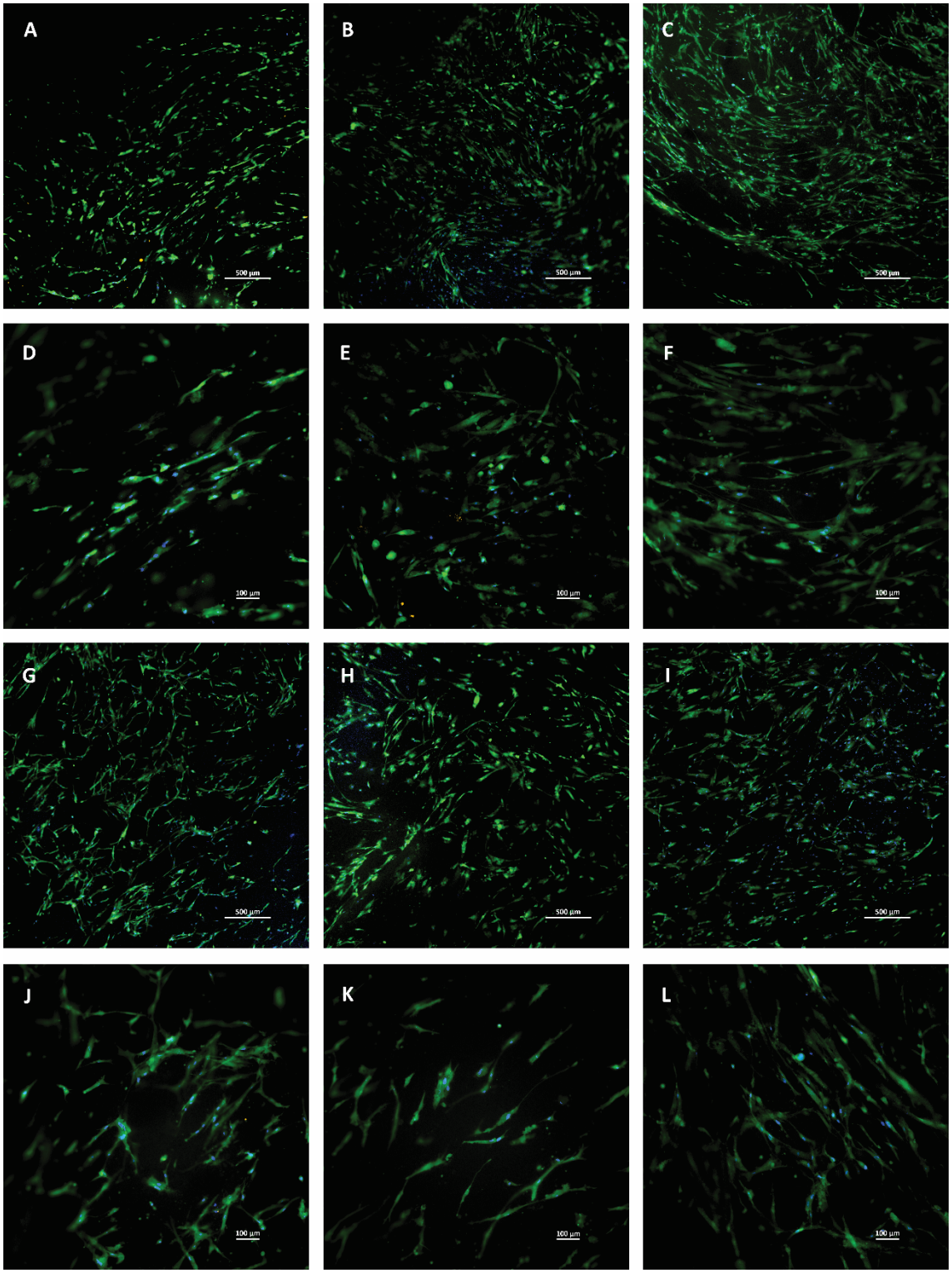

Figure 10. *Live-dead staining of hBM-dMSCs cultured on different fibrin membranes.* Live cells are shown in green, dead cells in yellow, and nuclei are blue. Images were taken at 4× **(A-C**), and **(G-I)**, or at 10× **(D-E)** and **(J-L)** magnification and the scale bars represent either 500 (A-C, and G-I) or 100 (D-F, and I-L) µm. The fibrin membrane

groups, isolated from cryoprecipitate, are the following: C1 **(A, D)**; C2 **(B, E)**; C3 **(C, F)**; C4 **(G, J)**; Sn **(H, K)**; and Control **(I, L)** (89).

4.4. Viability of hBM-dMSCs cultured on the fibrin membranes

We investigated the cell attachment and viability on fibrin membranes with XTT measurements. After one day, viability was examined to obtain information about cell adhesion onto different membranes. There was no significant difference in cell attachment between the groups (Figure 11). After seven days, cell proliferation was measured on the membranes. No significant difference was observed; however, there was an increasing tendency in cell viability along the C2, C3 and C4 groups. We found no difference in cell viability between the first and seventh day, either (Figure 11).

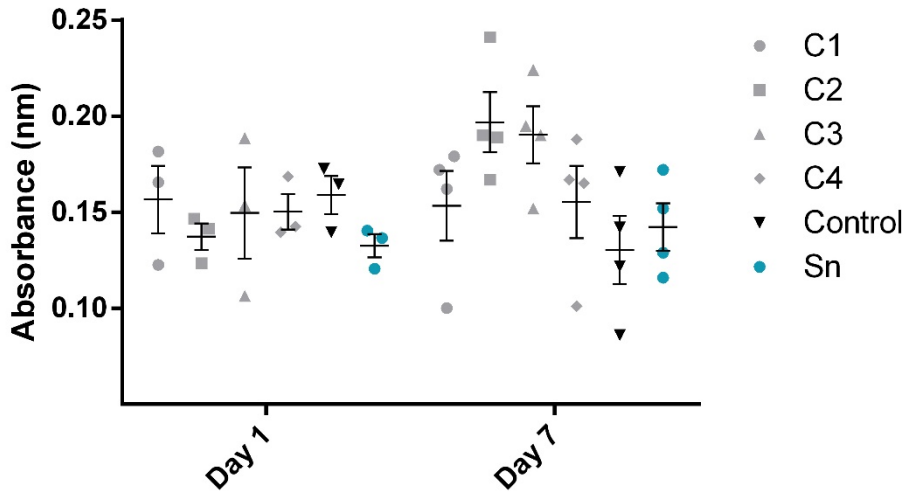

Figure 11. *The viability of hBM-dMSCs cultured on the fibrin membranes.* Cell attachment after one day and cell proliferation after seven days of culture on fibrin membranes. The membranes were isolated from cryoprecipitate, which was resolubilized in 10 mL (C1), 20 mL (C2), 30 mL (C3), and 40 mL (C4) plasma, from the supernatant (Sn), which was collected from above the cryoprecipitate and pooled, and from plasma, which was used as a control (n = 3 on day 1 and n = 4 on day 7). One-way analysis of variance (ANOVA) with Tukey's post hoc test (89).

4.5. Assessment of albumin-LPA complex formation with FTIR

To evaluate if the complex formation occurs between LPA and HSA, we investigated structure-related chemical changes with the use of FTIR. The FTIR measurement results are shown in (Figure 12). The absorbances were normalized to the 2916 cm^{-1} peak in the case of LPA species, and the spectra were vertically shifted for a better understanding and to prevent overlapping. Figure 12A shows the FTIR spectra of native 18:2, 18:1, and 16:0 LPA species, whereas the spectra of HSA and HSA-bound 18:2, 18:1, and 16:0 LPA are shown in Figure 12B. These absorbances were normalized to the absorbance peak at 1648 cm^{-1}.

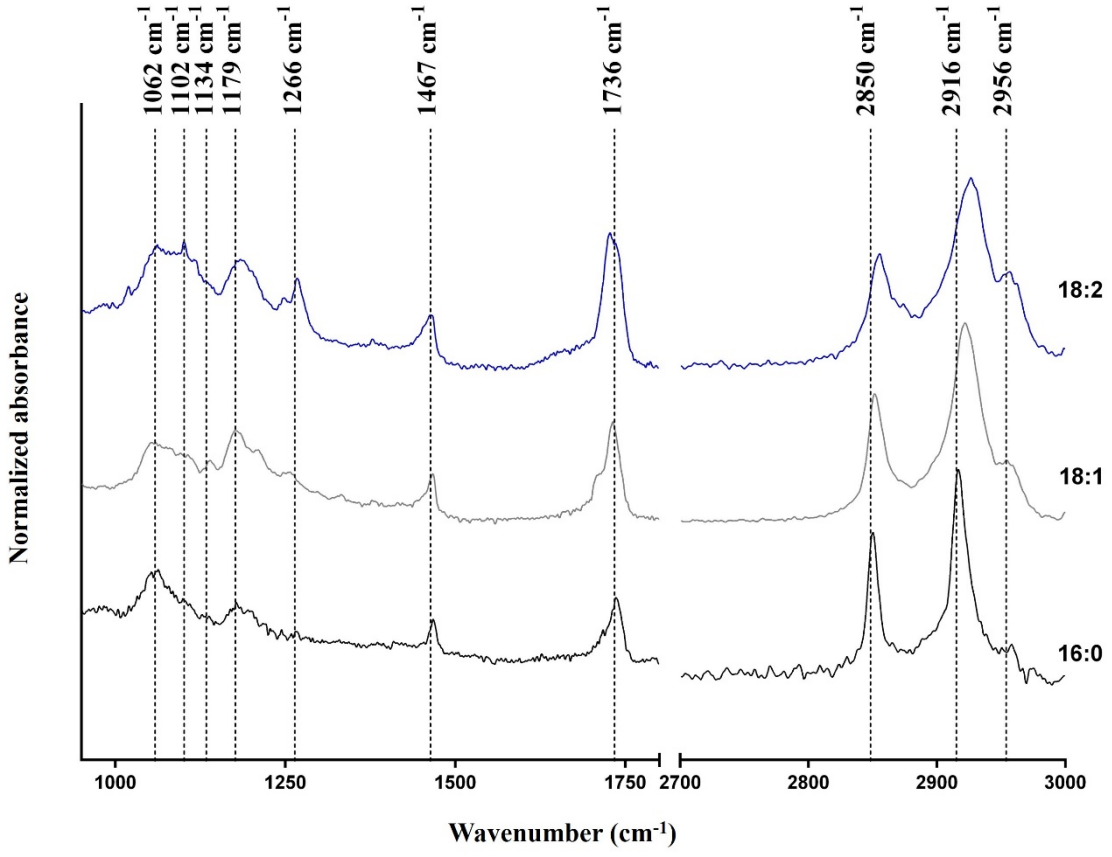

(A)

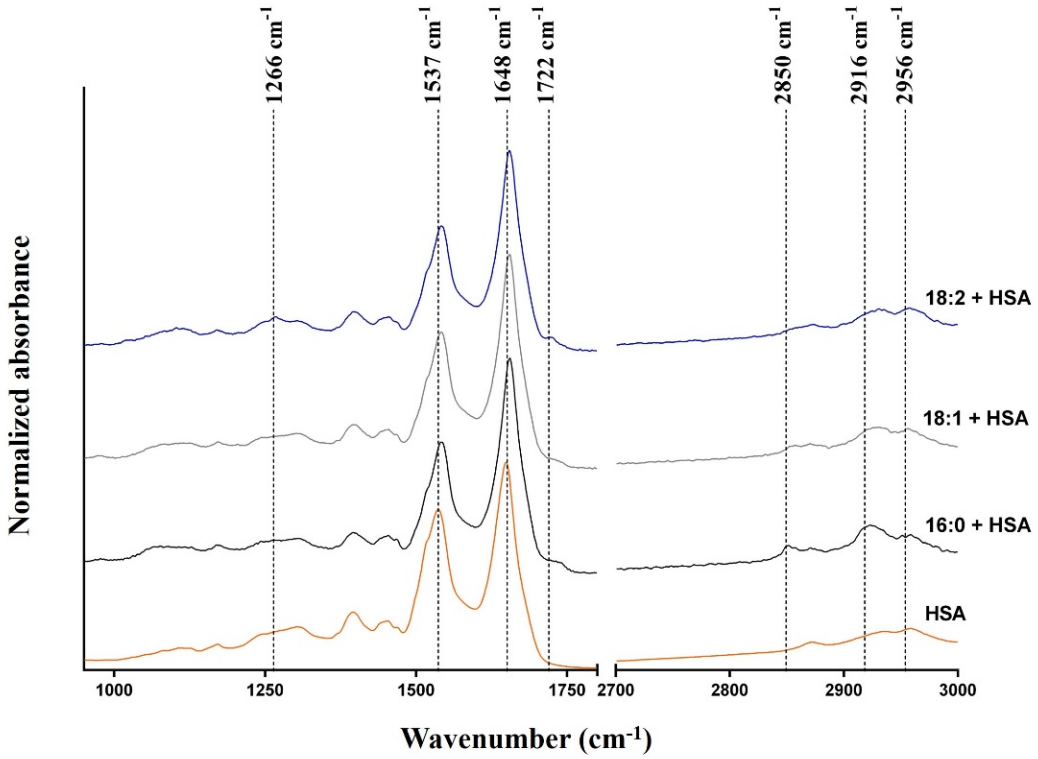

(B)

Figure 12. *FTIR spectra of native and HSA-bound LPA species and native HSA.* Native 16:0 LPA is shown at the bottom, 18:1 in the middle, and 18:2 at the top of the image **(A)**. The bottom line shows the FTIR spectra of native HSA and, in a vertical sequence, HSA-bound 16:0, 18:1, and 18:2 LPA species are shown **(B)** (91).

In the case of the FTIR spectra of LPA species, the main absorbances were characteristic for the CH_2 groups (2916–2926 cm^{-1}), the C=O groups (1736 cm^{-1}), C-O bonds (1179 cm^{-1}), and P-O-C bonds (1062 cm^{-1}). In the case of HSA, the two characteristic bonds were the amide I (1648 cm^{-1}) and amide II (1537 cm^{-1}) absorption bands.

4.6. Effects of LPA species on hBM-dMSCs proliferation

We performed XTT measurements to investigate the possible cytotoxicity and to determine the effects of 18:1, 18:2, and 16:0 LPA on the proliferation of hBM-dMSCs. The cells were treated with increasing concentrations of phospholipids alone or in combination with HSA. After 24 h of treatment, none of the three LPA species showed cytotoxic effects up to 10 µM concentration. 18:1 LPA in 1, 3, and 10 µM concentrations

significantly increased cell proliferation compared to the control group, but solely when administered in the presence of HSA (Figure 13A). In addition, 18:2 LPA significantly enhanced the proliferation of hBM-dMSCs in combination with HSA in 1, 3, and 10 µM and when examined alone in 3 and 10 µM concentrations (Figure 13B). A significant elevation in cell proliferation was caused by 0.3, 1, 3, and 10 µM 16:0 LPA treatment, exclusively in combination with HSA (Figure 13C). Interestingly, among the examined three LPA species, only 18:2 LPA in 3 and 10 µM concentrations significantly increased cell proliferation when administered without HSA (Figure 13B).

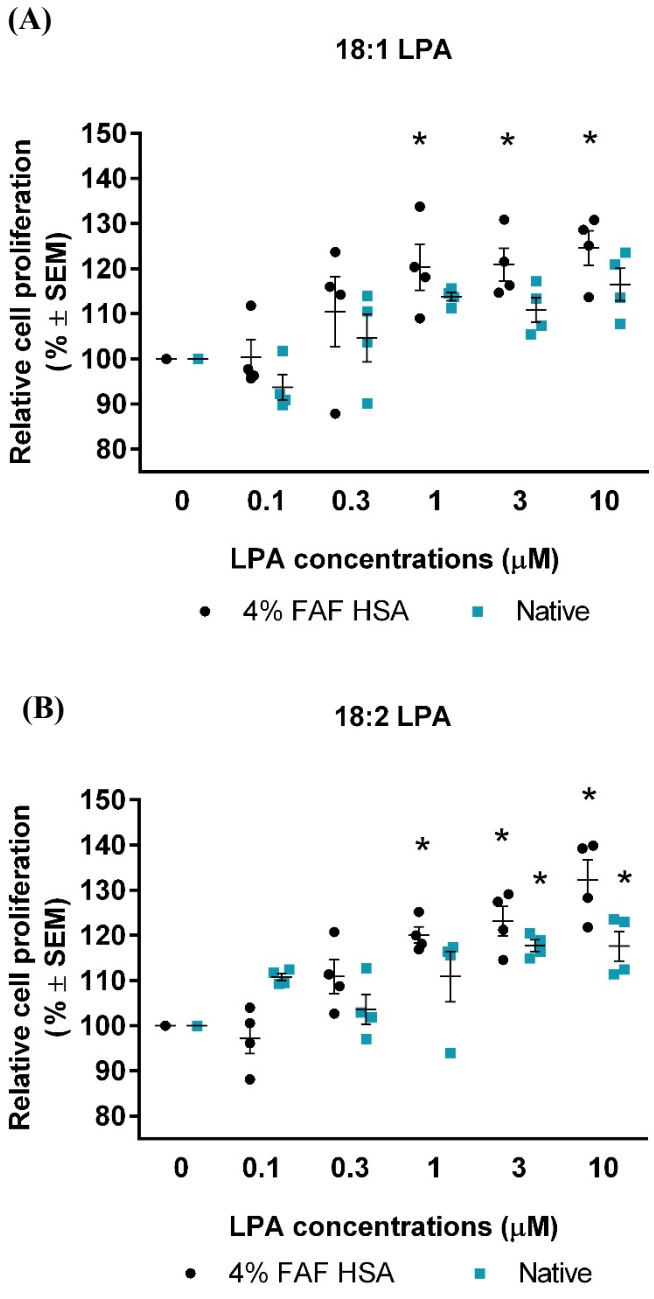

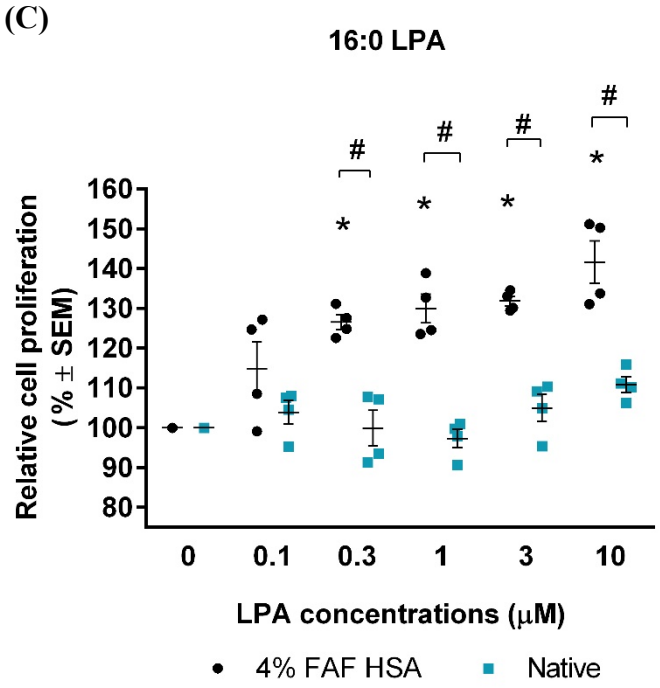

Figure 13. *The effect of LPA species on hBM-dMSCs proliferation.* Relative cell proliferation after 18:1 **(A)**, 18:2 **(B)** and 16:0 **(C)** LPA treatment in combination with HSA (4% FFA HSA, black dots) or alone (native, blue squares). (* $p < 0.05$ vs. Control (0 μM LPA), # $p < 0.05$, n = 4 in each group, two-way ANOVA, followed by Tukey's multiple comparison test). Data are presented as % of Control and mean ± SEM (91).

4.7. The effect of LPA species on the migration of hBM-dMSCs

To investigate if 18:1, 18:2, or 16:0 LPA influence the migration of the hBM-dMSCs, wound healing assay experiments were performed. The representative figure of the procedure is shown below (Figure 14). The initial scratch area did not differ significantly in the treatment groups. The cells did not completely fill the gaps after 24 hours of treatment. However, none of the three LPA species significantly enhanced cell migration, neither 12 h nor 24 h after treatment, compared with the control group. There was also no relevant improvement in cell migration between the HSA-bound LPA and the native LPA-treated groups (Figure 15). HSA-bound 16:0 LPA in a 10 μM concentration significantly improved the migration of the cells after 12 h, compared to the 10 μM native LPA, and the 1 μM HSA-bound groups. The difference disappeared after 24 h of treatment. After 24 hours the 3 μM HSA-bound LPA group differed significantly from the 10 μM native, and 1 μM HSA-bound LPA treatments (Figure 15C).

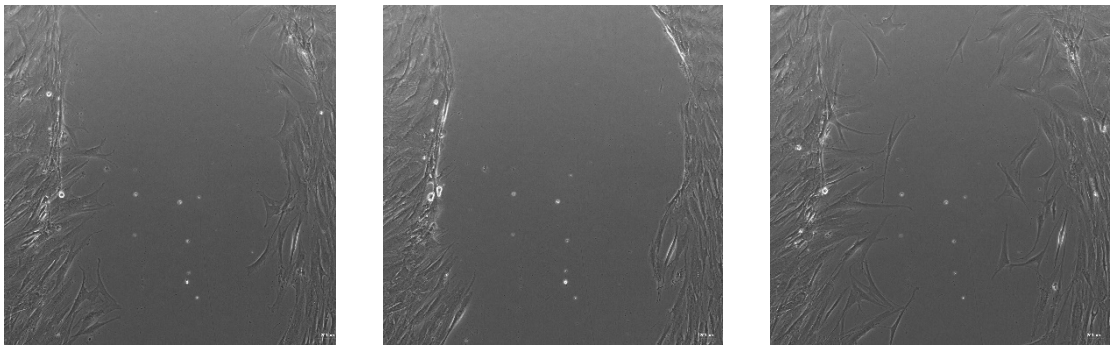

(**A**) (**B**) (**C**)

Figure 14. *Representative bright-field images of the in vitro wound healing assay.* The "wound" was created by a line scratch across the hBM-dMSCs monolayer (**A**). Images were analyzed after 12 h (**B**) and 24 h (**C**) of treatment. The images were taken in 10× magnification, and the scale bar represents 200 μm (91).

(A)

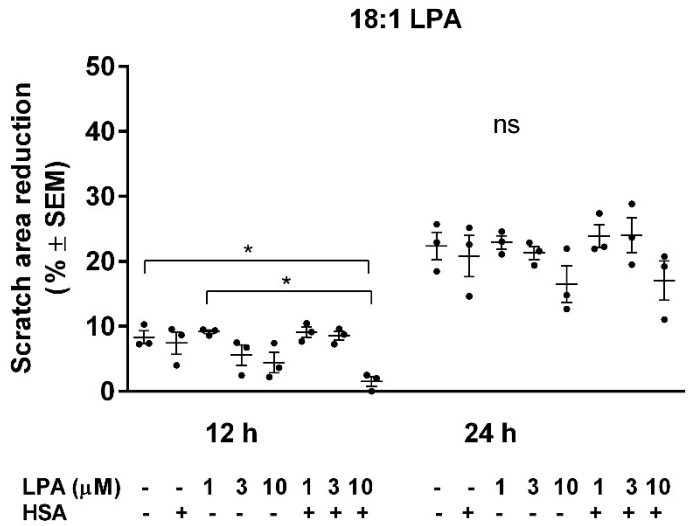

(B)

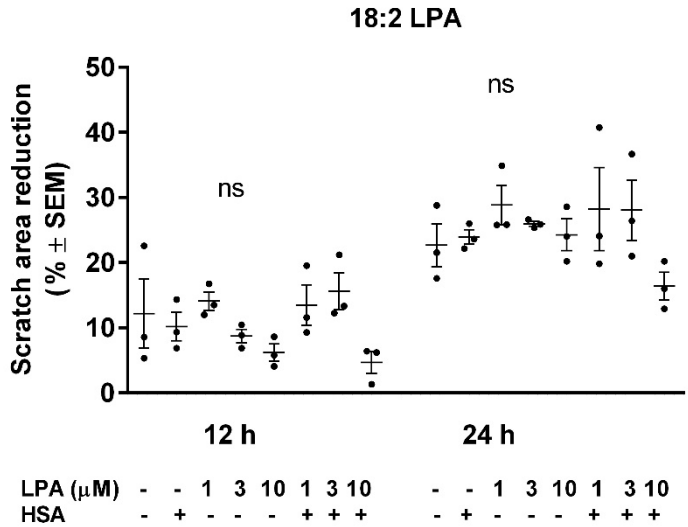

(C)

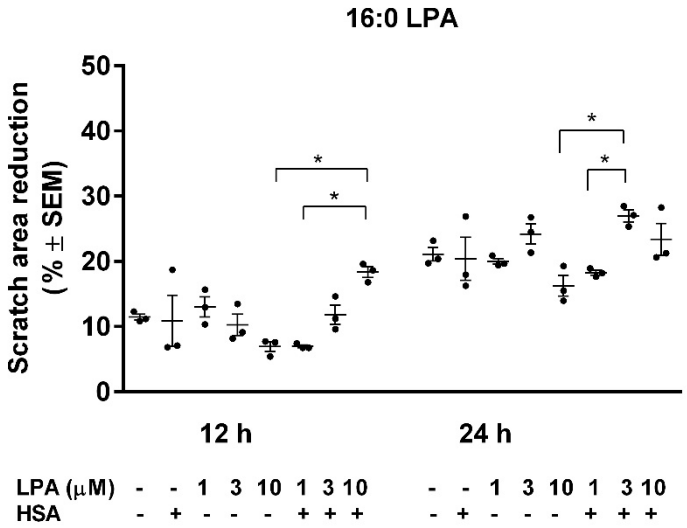

Figure 15. *Scratch area reduction (%) after treatment with* ***(A)*** *18:1,* ***(B)*** *18:2 and* ***(C)*** *16:0 LPA species for 12 and 24 h.* hBM-dMSCs were treated with different LPA species in 1 μM, 3 μM, and 10 μM concentrations alone or combination with HSA (* $p < 0.05$, n = 3, One-way ANOVA followed by Tukey's multiple comparison test). Data are presented as mean ± SEM. The migration rate is expressed as the percentage of area reduction (91).

4.8. Cell attachment capacity of LPA and HSA-coated DBMs

Attachment of hBM-dMSCs was examined on differently coated DBMs after one day and seven days of incubation. The results show that cells attached to the surface of bone grafts in every group, but no significant difference was observed between the groups after one day and seven days either. However, an increasing tendency can be seen in cell attachment in the case of treated DBMs compared to Control (Figure 16).

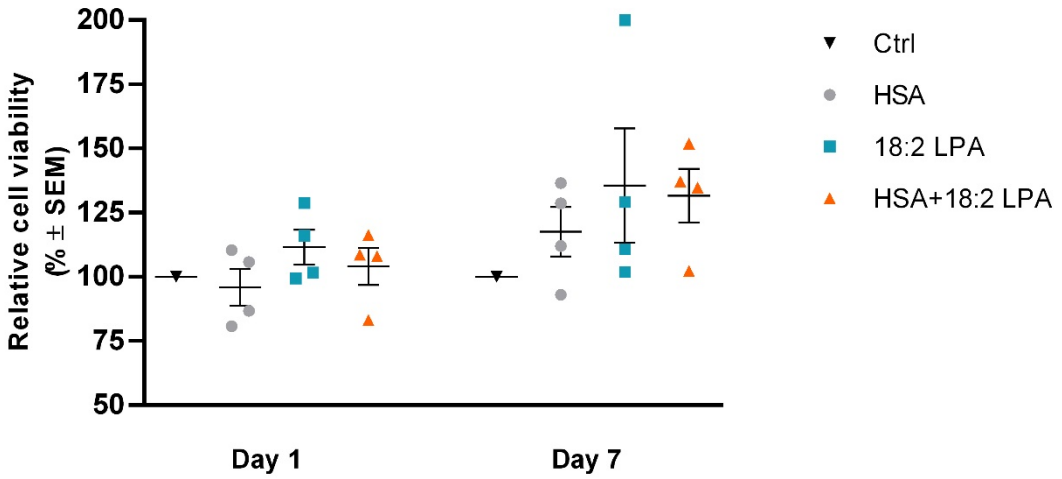

Figure 16. *Relative viability of hBM-dMSCs seeded on different DBMs after one and seven days of incubation.* DBMs were coated with either PBS (Ctrl), HSA, 18:2 LPA, or HSA and 18:2 LPA together. (n=4 in each group, One-way ANOVA followed by Tukey's multiple comparison test). Data are presented as % of Control and mean ± SEM (A.M., 2023. Unpublished work).

5. Discussion

Although bone regeneration is one of the regenerative processes that generally lead to complete recovery, in certain fractures, defects or ageing-related reduced healing capabilities, it can be advantageous to enhance the union of bone. In this type of enhanced bone regeneration, the gap between the damaged bone fragments needs to be filled with a functional biomaterial that acts as a physical 3D microenvironment for the attachment, proliferation, and migration of the surrounding cells (4) in order to help remodeling. Soft tissue implants, such as membranes and DBMs, are widely used in TERM and are suitable candidates for bone regenerative applications (5). Our aim within regenerative medicine is the development of a soft tissue implant that effectively promotes bone regeneration and new bone formation. Therefore, we examined fibrin membranes and DBMs containing LPA and HSA in terms of scaffold development.

Fibrin membranes were prepared from fresh frozen plasma and cryoprecipitate. When frozen plasma is thawed and centrifuged, some of the blood components can be enriched in the precipitate due to reduced solubility at lower temperatures. Although, theoretically, plasma isolated by plasmapheresis does not contain any cellular elements (92), in our experiments, we found a small amount of platelets, leukocytes, and red blood cells in the samples. The control plasma contained approximately 10×10^9/L platelets. The platelet count in plasma significantly depends on the isolation method. For instance, manually isolated platelet-poor plasma is reported to contain 34.5×10^9/L platelets (93), while the average whole blood platelet count is $150\text{-}450\times10^9$/L (94). We also found that the number of the measured platelets increased with the increasing fibrinogen concentration of cryoprecipitate. Platelet number is important, as during activation, they release platelet-derived growth factors, which can be entrapped in the fibrin network, and thus promote regeneration. We observed no significant differences in the concentration of leukocytes and red blood cells between the groups, however, their level showed a tendency to increase in the more concentrated cryoprecipitate samples. The presence of leukocytes and red blood cells in the samples may only be due to centrifugation, not because of the solvent properties, as they were not reported to be enriched in cryoprecipitate. Haemoglobin level was investigated to obtain information about the amount of disrupted red blood cells, but it was only detectable in the C1 group.

From the viewpoint of developing a fibrin membrane, the most essential protein component of cryoprecipitate is fibrinogen. According to our results, the fibrinogen level of cryoprecipitate was higher when the cryoprecipitate was dissolved in decreasing amounts of plasma. Besides its previously mentioned beneficial regenerative properties, fibrinogen concentration also has an impact on the thickness of the prepared membranes. ALP enzyme catalyzes the dephosphorylation of proteins, nucleic acids, and small molecules and can be found in numerous tissues; thus, it is often used as a biomarker (95). Furthermore, ALP regulates bone mineralization. It increases local inorganic phosphate concentration and reduces extracellular pyrophosphate, an inhibitor for mineral formation (96). In our experiments, all samples showed ALP activity, although no significant difference was observed. The total protein concentration was also slightly but significantly affected by cryoprecipitate isolation, which may be due to fibrinogen. Albumin concentration, despite its good water solubility, also showed a mild decreasing tendency with decreasing cryoprecipitate concentration.

Greater membrane thickness can improve the application of the scaffold. Fibrin membranes were prepared in 24-well culture plates; thus, their diameter can be considered identical. Weight measurement data of the freeze-dried membranes demonstrated that membranes isolated from more concentrated cryoprecipitate result in higher thickness. The decomposition of the fibrin membranes is also an important factor, which can further be improved with the addition of plasminogen inhibitors, as in the medical device called the duploject system.

One of the most important criteria for scaffold development is that it should have good biocompatibility and enable cellular attachment and growth (97). Therefore, we investigated the attachment of hBM-dMSCs onto the surface of fibrin membranes with different thicknesses. Cells were visualized with live-dead staining, and the amount of the attached cells was quantified using XTT cell viability assay. The cells attached to the membranes confirm their structure to be viable for cells. However, neither the microscopic images nor the XTT measurements showed significant differences between the groups. The structures were considered to be thicker with increasing fibrinogen concentration and were suitable to be sutured (47), but the weight-bearing limitations of this membrane posed a serious obstacle to being used as a scaffold that can enhance bone regeneration. The fibrin-containing scaffold was further developed to become a soft tissue

implant. In this study the fibrin network was incorporated into freeze-dried crosslinked hyaluronic acid. We found that fibrin-containing crosslinked scaffolds had larger cell and extracellular matrix content and developed more blood vessels 12 weeks after implantation compared to the control implants, which is favorable regarding remodeling. However, our measurements also showed that crosslinking resulted slower degradation. There was no significant difference in the weights of the implants of the same scaffold type even after 12 weeks of implantation. The fibrin content further enhanced the resistance of the scaffolds to degradation. Fibrin-containing scaffolds showed larger weights compared to the native implants (2). Biodegradability is a key requirement of any scaffold since the aim of TE is to allow the body's own cells to replace the implanted scaffold over time (3). Therefore, we concluded that the fibrin membrane was not suitable to be used for our purposes as a bone replacement implant, coating or additive to enhance bone remodeling.

The other scaffold type we investigated during development was HSA and LPA coated DBM. To ensure that HSA and LPA can be homogenously and effectively mixed in an aqueous solution, FTIR measurements were carried out to investigate whether the two components can be identified and if there is a visible complex formation between LPA and HSA under our experimental settings. The IR spectra were assessed for the three physiologically most abundant 16:0, 18:1, and 18:2 LPA derivatives, we measured the wavenumber of the characteristic absorbances. During measurements, we used fatty acid-free HSA; thus, it did not contain any complex-forming fatty acid molecules. The LPA was solubilized in methanol and water to avoid any secondary binding and to ensure the purity of the reagents for spectroscopic purposes. The stretching of the CH_2 groups is visible in the 2916–2926 cm^{-1} range and around 2850 cm^{-1}. The CH_2 deformation vibrations occur at 1467 cm^{-1} (98), and at 1736 cm^{-1}, C=O stretching is visible (99). The absorbance at 1266 cm^{-1} has been described as the peak of the PO_2 asymmetric stretching vibration. However, this absorption is more profound in the spectrum of 18:2 LPA but should also appear in the spectra of 18:1 and 16:0 species. Alternatively, this band can result from the CH rocking, which is visible in the case of double bonds and is likely to be more intense in the case of 18:2 LPA due to the two double bonds (100). The purity of LPA 18:1 and 18:2 is in the 90 % range; thus, it may also be an acyl isomer impurity. The P-O-C and C-O bonds appear at 1062 cm^{-1} and 1179 cm^{-1}, respectively (101). Both CH_2

stretching absorbances shifted towards higher wavenumbers in the case of LPA derivatives, with an 18-carbon-atom acyl chain length compared with the 16-carbon-atom acyl chain length LPA. The increased CH_2 stretching frequencies indicate the higher disorder of the chains caused by the presence of double bonds in the acyl chains. The LPA species are known to form complexes with HSA in a 1:3 HSA:LPA ratio (64). Thus, we measured the formed complexes using FTIR to investigate whether absorbance shifting occurred. HSA peaks dominate in the spectrum compared to the LPA peaks, which is presumably due to the significant difference in the molecular weights of the components. The two prominent characteristic bands for albumin are the amide I and II bands at 1648 cm^{-1} and at 1537 cm^{-1} (102, 103). According to our evaluation, there was a slight spectral shift of the amide I band in the presence of LPA. The spectral shift was 1 cm^{-1} in the case of albumin-bound 18:1 LPA and 3 cm^{-1} in the case of 18:2 and 16:0 LPA variants. These shifts indicate a subtle change in the secondary structure while preserving the overall alpha-helical nature of the protein. A similar variation was observed in the case of the amide II band. These spectral changes in the amide bands might indicate the binding of LPA species to HSA.

As it was mentioned earlier, the proliferation of different bone cells plays a vital role during fracture healing (5). In a previous study, Chen *et al.* showed that LPA protects hBM-dMSCs against hypoxia and serum deprivation-induced apoptosis *in vitro*, indicating that LPA is a potent survival factor for hBM-dMSCs in bone repair applications (75). In addition, LPA was observed to promote H_2O_2-induced autophagy (76), the effect of which was shown to play an important role in cell survival (104). These findings make LPA a promising candidate to improve the viability and proliferation of hBM-dMSCs during bone healing. Our cell viability measurement data demonstrate that 18:1, 18:2, and 16:0 LPA species are non-toxic for hBM-dMSCs up to 10 μM concentration. Although there is evidence for the advantages of using LPA in bone regenerative medicine (4, 81), there are still some challenges with the *in vivo* application of LPA. LPA is easily degraded *in vivo* by lipid phosphate phosphatases (87); thus, LPA requires a carrier that allows the successful delivery of the lipid. Albumin besides acting as a carrier protein for metal ions, fatty acids, pharmacons, and growth factors, is also known to promote the viability and proliferation of stem cells (34). In our experiments, all the three tested LPA species improved the proliferation of hBM-dMSCs, which effect was more pronounced when

administered in the presence of HSA. This finding supports our hypothesis that HSA might serve as an ideal carrier for LPA in bone regenerative applications. However, in our measurements HSA alone did not significantly enhance cell proliferation. This observation might be due to the fatty acid-free characteristic of the used HSA. In our experimental setup we aimed to reduce the variables to be able to focus on the potential effect of LPA and HSA exclusively and investigate if there is a synergistic effect between these two constituents due to the modification of the LPA distribution via complex formation with HSA.

Furthermore, 18:1 and 16:0 LPA species did not significantly improve cell proliferation without HSA. Interestingly, this effect appeared in the case of 18:2 LPA in 3 and 10 μM concentrations. The regulated signaling pathway during this LPA effect is not yet evaluated. However, it is possible that these LPA species need to be transported to their receptors for signaling pathway activation. The expression of $LPAR_{1,2,3,4,5}$ has been identified in human and murine MSCs. However, $LPAR_1$ was reported to be the most frequently detected type of LPA receptor in hBM-dMSCs (73). It is also known that each LPA receptor can be activated differently by the LPA species. For instance, $LPAR_3$ shows the highest reactivity with 18:1, 18:2, and 18:3 LPA, while $LPAR_1$ and $LPAR_2$ bind the naturally most abundant acyl-LPA species equally (105).

The proliferative effect of LPA seemed to be dose-dependent. The highest increments in cell proliferation were shown in the case of treatment with 18:2 LPA in 3 and 10 μM and 16:0 LPA in 0.3, 1, 3, and 10 μM concentrations.

LPA is known to mediate the migration of various cell types (106, 107), which might be in connection with the experienced, LPA-enhanced proliferation of the hBM-dMSCs. In a previous research article, Song *et al.* showed that LPA induced the migration of hBM-dMSCs (108). Thus, as our next step, we investigated whether the different LPA species in the presence or absence of HSA affect the migration of hBM-dMSCs. However, none of the three LPA species enhanced the cell migration significantly, neither 12 nor 24 h after treatment, compared to the control group. There was no remarkable difference between the HSA-bound LPA and the native LPA-treated groups either. Hence, it seems that, in our case, the viability-enhancing effect of LPA is not directly proportional to the migration in the case of hBM-dMSCs. However, the study's limitation lies in the small

number of values. It is also possible that the proliferation and migration-promoting effect of LPA occur through the activation of different signaling pathways. In accordance with the literature data, the migration-promoting effect of LPA requires the LPA_1-dependent activation of calmodulin-dependent protein kinase II (108). On the other hand, it is reported that LPA promoted the survival of BM-dMSCs trough the activation of G_i protein-coupled $LPA_{1/3}$ and extracellular signal-regulated kinase pathway (75, 76, 109).

According to viability testing and cell proliferation results, 10 μM 18:2 LPA seemed to be the most effective for further utilization. Therefore, we coated DBMs with either 18:2 LPA, HSA, or with 18:2 LPA and HSA in a 3:1 molar ratio. For the soaking stock solution, we chose 10× of the preferred final concentration based on previously published literature data (71). Thereafter, we measured the attachment of hBM-dMSCs seeded on freeze-dried, variously treated DBMs with XTT assay. The cells attached to the bone grafts and an increasing tendency was observed in the number of the attached cells when they were seeded on treated scaffolds, compared to the control group, especially after seven days of incubation. However, no significant difference was observed between the different groups.

6. Conclusions

Our aim during the experiments was the *in vitro* investigation of soft tissue implants for subsequent *in vivo* utilization for bone regeneration. Fibrin membranes isolated from fresh frozen plasma and cryoprecipitates and demineralized bone matrices supplemented with LPA and HSA were examined. The cellular element and protein content of FFP and cryoprecipitate with different concentrations were measured. The weights of the prepared fibrin membranes were compared, and their biocompatibility was tested by the examination of the attached cells using a microscopic technique and quantified with cell viability assay as well. Furthermore, for LPA and HSA containing DBM development, complex formation between LPA and HSA was analyzed, and the toxicity profile of various concentrations of 16:0, 18:1, and 18:2 native and HSA-bound LPA species was also investigated. In addition, we studied if the presence of LPA and/or HSA is beneficial for the proliferation, migration and attachment of hBM-dMSCs.

According to our results, it can be concluded that plasma products with increased fibrinogen and platelet concentration can be efficiently prepared from cryoprecipitate. At the same time, the level of the other measured components remained mainly similar. Fibrin membrane thickness increased with the increasing fibrin concentration of the membranes, which is favorable regarding TE-related applications. Microscopic analysis revealed that fibrin membranes are convenient for stem cell attachment, which is a necessary factor for proper scaffold implantation and one of the most important criteria of scaffold development. Quantification of the hBM-dMSCs attachment with XTT assay showed no significant difference between the various fibrin membrane groups, which indicates that membrane thickness does not influence the degree of cellular attachment or proliferation. The use of increased fibrin concentration may only lead to practical advantages, e.g., the mechanical properties or the ability to enable suturing of the scaffolds or to delay the degradation.

During IR measurements, we compared the characteristic peaks of HSA before and after the addition of the different LPA species to determine if any shifting of the absorbance wavelength of the characteristic peaks occurred. We found small spectral shifts of the amide I and II bands of HSA in the presence of all three tested LPA species, indicating subtle changes in the secondary structure of the HSA due to the binding of

LPA. These results prove that complex formation occurs between the components in an aqueous solution; thus, HSA can be used as a potential carrier for LPA in our further experiments. From cell viability measurement data, we concluded that the investigated 16:0, 18:1, and 18:2 LPA species are safe to be used up to 10 μM concentration due to their non-toxic characteristics in hBM-dMSCs. Furthermore, LPA promoted cell proliferation dose-dependently, in combination with HSA. Cell viability and proliferation results showed that 18:2 LPA in 10 μM concentration was the most effective either when administered alone or in the presence of HSA. Therefore, it seems to be a promising supplementation in TERM-related applications. Cell migration analysis showed no remarkable enhancement after LPA treatment, with or without HSA. Thus, it can be said that the observed cell proliferative effect of LPA treatment is not directly in connection with the enhanced migration of hBM-dMSCs.

The *in vitro* analysis of fibrin membranes and supplemented DBMs showed that both scaffolds might be suitable for *in vivo* application. However, regarding bone regeneration, 18:2 LPA and HSA-coated DBMs seem to be the most promising candidates due to their high biocompatibility and hBM-dMSCs viability and proliferation-promoting properties. Our experiments might contribute to the development of a new, more effective, innovatively manufactured bone replacement product that enables faster and superior regeneration, thus shortening healing time and lowering the risk of further injuries.

7. Summary

Nowadays, the number of bone diseases and defects is increasing; thus, the repair or replacement of damaged or lost bone tissue has an outstanding role in RM (7). Scaffolds are extensively studied for bone regeneration, but treating significant bone loss remains a challenge. Therefore, we aimed to develop a soft tissue implant that promotes stronger new bone formation after implantation. In the present work, fibrin membranes and DBMs supplemented with LPA and HSA were tested *in vitro.*

The use of fibrin in bone TE is favourable due to its excellent biocompatibility, controllable biodegradability, and cell or drug deliver ability (45). We investigated fibrin membranes isolated from FFP or cryoprecipitate. Membranes isolated from more concentrated cryoprecipitate resulted in higher thickness, which makes them superior during implantation. The hBM-dMSCs attached to the surface of the membranes prove their biocompatible structure and enable their *in vivo* utilization.

LPA not only regulates bone homeostasis but plays an important role during bone regeneration due to its multiple effects on bone cells, especially BMSCs and osteoblasts (73), which make the use of LPA promising in RM. FTIR measurements confirmed complex formation between LPA and HSA when administered in a 3:1 molar ratio. This complex formation might have a key role in the successful delivery of the lipid. Biocompatibility testing showed that LPA had no cytotoxic effect up to 10 µM concentration. Furthermore, LPA promoted the proliferation of hBM-dMSCs dose-dependently, which is a vital step during bone healing. According to our measurements, 18:2 LPA seemed to be the most effective, primarily when used in combination with HSA. The hBM-dMSCs were also able to attach to DBMs when they were coated with HSA. However, cell attachment showed an increasing tendency when DBMs were treated with 18:2 LPA or with 18:2 LPA and HSA in combination.

In summary, in the present work, we have demonstrated that cryoprecipitate isolation is an efficient method for preparing plasma products with increased fibrinogen concentration. According to our experiments, the isolated membranes may act as a base for a new innovative product for TE. Furthermore, we proved that LPA is suitable for increasing cell viability alone and in combination with HSA *in vitro*, which may be a useful supplementation in TERM-related applications.

8. References

1. Hinsenkamp A, Kardos D, Lacza Z, Hornyák I. A Practical Guide to Class IIa Medical Device Development. Applied Sciences. 2020;10(10):3638.
2. Hinsenkamp A, Fülöp Á, Hricisák L, Pál É, Kun K, Majer A, Varga V, Lacza Z, Hornyák I. Application of Injectable, Crosslinked, Fibrin-Containing Hyaluronic Acid Scaffolds for In Vivo Remodeling. J Funct Biomater. 2022;13(3).
3. O'Brien FJ. Biomaterials & scaffolds for tissue engineering. Materials Today. 2011;14(3):88-95.
4. Bosetti M, Borrone A, Leigheb M, Shastri VP, Cannas M. (*) Injectable Graft Substitute Active on Bone Tissue Regeneration. Tissue Eng Part A. 2017;23(23-24):1413-1422.
5. O'Keefe RJ, Mao J. Bone tissue engineering and regeneration: from discovery to the clinic--an overview. Tissue Eng Part B Rev. 2011;17(6):389-392.
6. Oryan A, Monazzah S, Bigham-Sadegh A. Bone injury and fracture healing biology. Biomed Environ Sci. 2015;28(1):57-71.
7. Ansari M. Bone tissue regeneration: biology, strategies and interface studies. Prog Biomater. 2019;8(4):223-237.
8. Lafuente-Gracia L, Borgiani E, Nasello G, Geris L. Towards in silico Models of the Inflammatory Response in Bone Fracture Healing. Front Bioeng Biotechnol. 2021;9:703725.
9. Fernández-Tresguerres-Hernández-Gil I, Alobera-Gracia MA, del-Canto-Pingarrón M, Blanco-Jerez L. Physiological bases of bone regeneration I. Histology and physiology of bone tissue. Med Oral Patol Oral Cir Bucal. 2006;11(1):E47-51.
10. Gibon E, Lu L, Goodman SB. Aging, inflammation, stem cells, and bone healing. Stem Cell Research & Therapy. 2016;7(1):44.
11. Office of the Surgeon G. Reports of the Surgeon General. Bone Health and Osteoporosis: A Report of the Surgeon General. Rockville (MD): Office of the Surgeon General (US); 2004.
12. Holzmann P, Niculescu-Morzsa E, Zwickl H, Halbwirth F, Pichler M, Matzner M, Gottsauner-Wolf F, Nehrer S. Investigation of bone allografts representing different steps of the bone bank procedure using the CAM-model. Altex. 2010;27(2):97-103.

13. Salgado AJ, Oliveira JM, Martins A, Teixeira FG, Silva NA, Neves NM, Sousa N, Reis RL. Tissue engineering and regenerative medicine: past, present, and future. Int Rev Neurobiol. 2013;108:1-33.
14. Ren X, Zhao M, Lash B, Martino MM, Julier Z. Growth Factor Engineering Strategies for Regenerative Medicine Applications. Front Bioeng Biotechnol. 2019;7:469.
15. Frey BM, Zeisberger SM, Hoerstrup SP. Tissue Engineering and Regenerative Medicine - New Initiatives for Individual Treatment Offers. Transfusion Medicine and Hemotherapy. 2016;43(5):318-320.
16. Sánchez A, Schimmang T, García-Sancho J. Cell and tissue therapy in regenerative medicine. Adv Exp Med Biol. 2012;741:89-102.
17. Bianco P, Robey PG, Simmons PJ. Mesenchymal stem cells: revisiting history, concepts, and assays. Cell Stem Cell. 2008;2(4):313-319.
18. Fu X, Liu G, Halim A, Ju Y, Luo Q, Song AG. Mesenchymal Stem Cell Migration and Tissue Repair. Cells. 2019;8(8).
19. Chan BP, Leong KW. Scaffolding in tissue engineering: general approaches and tissue-specific considerations. Eur Spine J. 2008;17 Suppl 4(Suppl 4):467-479.
20. Qiu YL, Chen X, Hou YL, Hou YJ, Tian SB, Chen YH, Yu L, Nie MH, Liu XQ. Characterization of different biodegradable scaffolds in tissue engineering. Mol Med Rep. 2019;19(5):4043-4056.
21. Macchiarini P, Jungebluth P, Go T, Asnaghi MA, Rees LE, Cogan TA, Dodson A, Martorell J, Bellini S, Parnigotto PP, Dickinson SC, Hollander AP, Mantero S, Conconi MT, Birchall MA. Clinical transplantation of a tissue-engineered airway. Lancet. 2008;372(9655):2023-2030.
22. Atala A, Bauer SB, Soker S, Yoo JJ, Retik AB. Tissue-engineered autologous bladders for patients needing cystoplasty. Lancet. 2006;367(9518):1241-1246.
23. Sola A, Bertacchini J, D'Avella D, Anselmi L, Maraldi T, Marmiroli S, Messori M. Development of solvent-casting particulate leaching (SCPL) polymer scaffolds as improved three-dimensional supports to mimic the bone marrow niche. Mater Sci Eng C Mater Biol Appl. 2019;96:153-165.
24. Brougham CM, Levingstone TJ, Shen N, Cooney GM, Jockenhoevel S, Flanagan TC, O'Brien FJ. Freeze-Drying as a Novel Biofabrication Method for Achieving a

Controlled Microarchitecture within Large, Complex Natural Biomaterial Scaffolds. Adv Healthc Mater. 2017;6(21).

25. Song P, Zhou C, Fan H, Zhang B, Pei X, Fan Y, Jiang Q, Bao R, Yang Q, Dong Z, Zhang X. Novel 3D porous biocomposite scaffolds fabricated by fused deposition modeling and gas foaming combined technology. Composites Part B: Engineering. 2018;152:151-159.
26. Sampath Kumar TS, Yogeshwar Chakrapani V. Electrospun 3D Scaffolds for Tissue Regeneration. Adv Exp Med Biol. 2018;1078:29-47.
27. Gay S, Lefebvre G, Bonnin M, Nottelet B, Boury F, Gibaud A, Calvignac B. PLA scaffolds production from Thermally Induced Phase Separation: Effect of process parameters and development of an environmentally improved route assisted by supercritical carbon dioxide. The Journal of Supercritical Fluids. 2018;136:123-135.
28. Xu Y, Wang X. Application of 3D biomimetic models in drug delivery and regenerative medicine. Curr Pharm Des. 2015;21(12):1618-1626.
29. Mazzoni E, Iaquinta MR, Lanzillotti C, Mazziotta C, Maritati M, Montesi M, Sprio S, Tampieri A, Tognon M, Martini F. Bioactive Materials for Soft Tissue Repair. Front Bioeng Biotechnol. 2021;9:613787.
30. Silva SS, Rodrigues LC, Fernandes EM, Reis RL. Chapter 6 - Biopolymer membranes in tissue engineering. In: de Moraes MA, da Silva CF, Vieira RS, editors. Biopolymer Membranes and Films: Elsevier; 2020. p. 141-163.
31. Dimitriou R, Mataliotakis GI, Calori GM, Giannoudis PV. The role of barrier membranes for guided bone regeneration and restoration of large bone defects: current experimental and clinical evidence. BMC Med. 2012;10:81.
32. Gruskin E, Doll BA, Futrell FW, Schmitz JP, Hollinger JO. Demineralized bone matrix in bone repair: history and use. Adv Drug Deliv Rev. 2012;64(12):1063-1077.
33. Zhang H, Yang L, Yang XG, Wang F, Feng JT, Hua KC, Li Q, Hu YC. Demineralized Bone Matrix Carriers and their Clinical Applications: An Overview. Orthop Surg. 2019;11(5):725-737.
34. Weszl M, Skaliczki G, Cselenyák A, Kiss L, Major T, Schandl K, Bognár E, Stadler G, Peterbauer A, Csönge L, Lacza Z. Freeze-dried human serum albumin improves the adherence and proliferation of mesenchymal stem cells on mineralized human bone allografts. J Orthop Res. 2012;30(3):489-496.

35. Horváthy DB, Vácz G, Szabó T, Szigyártó IC, Toró I, Vámos B, Hornyák I, Renner K, Klára T, Szabó BT, Dobó-Nagy C, Doros A, Lacza Z. Serum albumin coating of demineralized bone matrix results in stronger new bone formation. J Biomed Mater Res B Appl Biomater. 2016;104(1):126-132.
36. Skaliczki G, Schandl K, Weszl M, Major T, Kovács M, Skaliczki J, Szendrői M, Dobó-Nagy C, Lacza Z. Serum albumin enhances bone healing in a nonunion femoral defect model in rats: a computer tomography micromorphometry study. Int Orthop. 2013;37(4):741-745.
37. Horváthy DB, Schandl K, Schwarz CM, Renner K, Hornyák I, Szabó BT, Niculescu-Morzsa E, Nehrer S, Dobó-Nagy C, Doros A, Lacza Z. Serum albumin-coated bone allograft (BoneAlbumin) results in faster bone formation and mechanically stronger bone in aging rats. J Tissue Eng Regen Med. 2019;13(3):416-422.
38. Kattula S, Byrnes JR, Wolberg AS. Fibrinogen and Fibrin in Hemostasis and Thrombosis. Arterioscler Thromb Vasc Biol. 2017;37(3):e13-e21.
39. John MJ, Byreddy P, Modak K, Makkar M. Congenital Fibrinogen Deficiency in India and Role of Human Fibrinogen Concentrate. Acta Haematologica. 2021;144:1-8.
40. Schulz PM, Gehringer W, Nöhring S, Müller S, Schmidt T, Kekeiss-Schertler S, Solomon C, Pock K, Römisch J. Biochemical characterization, stability, and pathogen safety of a new fibrinogen concentrate (fibryga(®)). Biologicals. 2018;52:72-77.
41. Brennan M. Fibrin glue. Blood Reviews. 1991;5(4):240-244.
42. Sacchi V, Mittermayr R, Hartinger J, Martino MM, Lorentz KM, Wolbank S, Hofmann A, Largo RA, Marschall JS, Groppa E, Gianni-Barrera R, Ehrbar M, Hubbell JA, Redl H, Banfi A. Long-lasting fibrin matrices ensure stable and functional angiogenesis by highly tunable, sustained delivery of recombinant VEGF164. Proc Natl Acad Sci U S A. 2014;111(19):6952-6957.
43. Sabatini L, Trecci A, Imarisio D, Uslenghi MD, Bianco G, Scagnelli R. Fibrin tissue adhesive reduces postoperative blood loss in total knee arthroplasty. J Orthop Traumatol. 2012;13(3):145-151.

44. Esposito F, Angileri FF, Kruse P, Cavallo LM, Solari D, Esposito V, Tomasello F, Cappabianca P. Fibrin Sealants in Dura Sealing: A Systematic Literature Review. PLoS One. 2016;11(4):e0151533.
45. Noori A, Ashrafi SJ, Vaez-Ghaemi R, Hatamian-Zaremi A, Webster TJ. A review of fibrin and fibrin composites for bone tissue engineering. Int J Nanomedicine. 2017;12:4937-4961.
46. Li Y, Meng H, Liu Y, Lee BP. Fibrin gel as an injectable biodegradable scaffold and cell carrier for tissue engineering. ScientificWorldJournal. 2015;2015:685690.
47. Kardos D, Hornyák I, Simon M, Hinsenkamp A, Marschall B, Várdai R, Kállay-Menyhárd A, Pinke B, Mészáros L, Kuten O, Nehrer S, Lacza Z. Biological and Mechanical Properties of Platelet-Rich Fibrin Membranes after Thermal Manipulation and Preparation in a Single-Syringe Closed System. International Journal of Molecular Sciences. 2018;19(11):3433.
48. Shainoff JR, Smejkal GB, DiBello PM, Mitkevich OV, Levy PJ, Dempfle CE, Lill H. Isolation and characterization of the fibrin intermediate arising from cleavage of one fibrinopeptide A from fibrinogen. J Biol Chem. 1996;271(39):24129-24137.
49. Wong HS, Curry NS. Cryoprecipitate transfusion: current perspectives. International Journal of Clinical Transfusion Medicine. 2016;4:89-97.
50. Mallis P, Gontika I, Dimou Z, Panagouli E, Zoidakis J, Makridakis M, Vlahou A, Georgiou E, Gkioka V, Stavropoulos-Giokas C, Michalopoulos E. Short Term Results of Fibrin Gel Obtained from Cord Blood Units: A Preliminary in Vitro Study. Bioengineering (Basel). 2019;6(3).
51. Liao HT, Marra KG, Rubin JP. Application of platelet-rich plasma and platelet-rich fibrin in fat grafting: basic science and literature review. Tissue Eng Part B Rev. 2014;20(4):267-276.
52. Moolenaar WH. Lysophosphatidic acid, a multifunctional phospholipid messenger. J Biol Chem. 1995;270(22):12949-12952.
53. Yung YC, Stoddard NC, Chun J. LPA receptor signaling: pharmacology, physiology, and pathophysiology. J Lipid Res. 2014;55(7):1192-1214.
54. Aoki J. Mechanisms of lysophosphatidic acid production. Semin Cell Dev Biol. 2004;15(5):477-489.

55. Aikawa S, Hashimoto T, Kano K, Aoki J. Lysophosphatidic acid as a lipid mediator with multiple biological actions. J Biochem. 2015;157(2):81-89.
56. Sano T, Baker D, Virag T, Wada A, Yatomi Y, Kobayashi T, Igarashi Y, Tigyi G. Multiple mechanisms linked to platelet activation result in lysophosphatidic acid and sphingosine 1-phosphate generation in blood. J Biol Chem. 2002;277(24):21197-21206.
57. Gerrard JM, Robinson P. Identification of the molecular species of lysophosphatidic acid produced when platelets are stimulated by thrombin. Biochimica et Biophysica Acta (BBA) - Lipids and Lipid Metabolism. 1989;1001(3):282-285.
58. Baker DL, Desiderio DM, Miller DD, Tolley B, Tigyi GJ. Direct Quantitative Analysis of Lysophosphatidic Acid Molecular Species by Stable Isotope Dilution Electrospray Ionization Liquid Chromatography–Mass Spectrometry. Analytical Biochemistry. 2001;292(2):287-295.
59. Pagès C, Simon MF, Valet P, Saulnier-Blache JS. Lysophosphatidic acid synthesis and release. Prostaglandins Other Lipid Mediat. 2001;64(1-4):1-10.
60. Liu YB, Kharode Y, Bodine PV, Yaworsky PJ, Robinson JA, Billiard J. LPA induces osteoblast differentiation through interplay of two receptors: LPA1 and LPA4. J Cell Biochem. 2010;109(4):794-800.
61. Mansell JP, Nowghani M, Pabbruwe M, Paterson IC, Smith AJ, Blom AW. Lysophosphatidic acid and calcitriol co-operate to promote human osteoblastogenesis: requirement of albumin-bound LPA. Prostaglandins Other Lipid Mediat. 2011;95(1-4):45-52.
62. Li YF, Li RS, Samuel SB, Cueto R, Li XY, Wang H, Yang XF. Lysophospholipids and their G protein-coupled receptors in atherosclerosis. Front Biosci (Landmark Ed). 2016;21(1):70-88.
63. Chen C, Ochoa LN, Kagan A, Chai H, Liang Z, Lin PH, Yao Q. Lysophosphatidic acid causes endothelial dysfunction in porcine coronary arteries and human coronary artery endothelial cells. Atherosclerosis. 2012;222(1):74-83.
64. Thumser AE, Voysey JE, Wilton DC. The binding of lysophospholipids to rat liver fatty acid-binding protein and albumin. Biochem J. 1994;301 (Pt 3)(Pt 3):801-806.
65. Michalczyk A, Budkowska M, Dołęgowska B, Chlubek D, Safranow K. Lysophosphatidic acid plasma concentrations in healthy subjects: circadian rhythm

and associations with demographic, anthropometric and biochemical parameters. Lipids Health Dis. 2017;16(1):140.

66. Hama K, Bandoh K, Kakehi Y, Aoki J, Arai H. Lysophosphatidic acid (LPA) receptors are activated differentially by biological fluids: possible role of LPA-binding proteins in activation of LPA receptors. FEBS Lett. 2002;523(1-3):187-192.
67. Meerschaert K, De Corte V, De Ville Y, Vandekerckhove J, Gettemans J. Gelsolin and functionally similar actin-binding proteins are regulated by lysophosphatidic acid. Embo j. 1998;17(20):5923-5932.
68. Blackburn J, Mansell JP. The emerging role of lysophosphatidic acid (LPA) in skeletal biology. Bone. 2012;50(3):756-762.
69. Salles JP, Laurencin-Dalicieux S, Conte-Auriol F, Briand-Mésange F, Gennero I. Bone defects in LPA receptor genetically modified mice. Biochim Biophys Acta. 2013;1831(1):93-98.
70. Karagiosis SA, Karin NJ. Lysophosphatidic acid induces osteocyte dendrite outgrowth. Biochem Biophys Res Commun. 2007;357(1):194-199.
71. Yu ZL, Jiao BF, Li ZB. Lysophosphatidic Acid Analogue rather than Lysophosphatidic Acid Promoted the Bone Formation In Vivo. Biomed Res Int. 2018;2018:7537630.
72. Kanehira M, Fujiwara T, Nakajima S, Okitsu Y, Onishi Y, Fukuhara N, Ichinohasama R, Okada Y, Harigae H. A Lysophosphatidic Acid Receptors 1 and 3 Axis Governs Cellular Senescence of Mesenchymal Stromal Cells and Promotes Growth and Vascularization of Multiple Myeloma. Stem Cells. 2016;35(3):739-753.
73. Wu X, Ma Y, Su N, Shen J, Zhang H, Wang H. Lysophosphatidic acid: Its role in bone cell biology and potential for use in bone regeneration. Prostaglandins Other Lipid Mediat. 2019;143:106335.
74. Lee MJ, Jeon ES, Lee JS, Cho M, Suh DS, Chang CL, Kim JH. Lysophosphatidic acid in malignant ascites stimulates migration of human mesenchymal stem cells. J Cell Biochem. 2008;104(2):499-510.
75. Chen J, Baydoun AR, Xu R, Deng L, Liu X, Zhu W, Shi L, Cong X, Hu S, Chen X. Lysophosphatidic acid protects mesenchymal stem cells against hypoxia and serum deprivation-induced apoptosis. Stem Cells. 2008;26(1):135-145.

76. Wang X-Y, Fan X-S, Cai L, Liu S, Cong X-F, Chen X. Lysophosphatidic acid rescues bone mesenchymal stem cells from hydrogen peroxide-induced apoptosis. Apoptosis. 2015;20(3):273-284.
77. Aki Y, Kondo A, Nakamura H, Togari A. Lysophosphatidic acid-stimulated interleukin-6 and -8 synthesis through LPA1 receptors on human osteoblasts. Archives of Oral Biology. 2008;53(3):207-213.
78. Lancaster S, Mansell JP. The role of lysophosphatidic acid on human osteoblast formation, maturation and the implications for bone health and disease. Clinical Lipidology. 2013;8(1):123-135.
79. Grey A, Chen Q, Callon K, Xu X, Reid IR, Cornish J. The phospholipids sphingosine-1-phosphate and lysophosphatidic acid prevent apoptosis in osteoblastic cells via a signaling pathway involving G(i) proteins and phosphatidylinositol-3 kinase. Endocrinology. 2002;143(12):4755-4763.
80. Dziak R, Yang BM, Leung BW, Li S, Marzec N, Margarone J, Bobek L. Effects of sphingosine-1-phosphate and lysophosphatidic acid on human osteoblastic cells. Prostaglandins Leukot Essent Fatty Acids. 2003;68(3):239-249.
81. Mansell JP, Barbour M, Moore C, Nowghani M, Pabbruwe M, Sjostrom T, Blom AW. The synergistic effects of lysophosphatidic acid receptor agonists and calcitriol on MG63 osteoblast maturation at titanium and hydroxyapatite surfaces. Biomaterials. 2010;31(2):199-206.
82. Alioli CA, Demesmay L, Laurencin-Dalacieux S, Beton N, Farlay D, Follet H, Saber A, Duboeuf F, Chun J, Rivera R, Bouvard D, Machuca-Gayet I, Salles JP, Gennero I, Peyruchaud O. Expression of the type 1 lysophosphatidic acid receptor in osteoblastic cell lineage controls both bone mineralization and osteocyte specification. Biochim Biophys Acta Mol Cell Biol Lipids. 2020;1865(8):158715.
83. Schaffler MB, Cheung W-Y, Majeska R, Kennedy O. Osteocytes: Master Orchestrators of Bone. Calcified Tissue International. 2014;94(1):5-24.
84. Hwang YS, Ma G-T, Park K-K, Chung W-Y. Lysophosphatidic acid stimulates osteoclast fusion through OC-STAMP and P2X7 receptor signaling. Journal of Bone and Mineral Metabolism. 2014;32(2):110-122.
85. Lapierre DM, Tanabe N, Pereverzev A, Spencer M, Shugg RP, Dixon SJ, Sims SM. Lysophosphatidic acid signals through multiple receptors in osteoclasts to elevate

cytosolic calcium concentration, evoke retraction, and promote cell survival. J Biol Chem. 2010;285(33):25792-25801.

86. Chen Y, Ramakrishnan DP, Ren B. Regulation of angiogenesis by phospholipid lysophosphatidic acid. Front Biosci (Landmark Ed). 2013;18(3):852-861.
87. Salous AK, Panchatcharam M, Sunkara M, Mueller P, Dong A, Wang Y, Graf GA, Smyth SS, Morris AJ. Mechanism of rapid elimination of lysophosphatidic acid and related lipids from the circulation of mice. Journal of lipid research. 2013;54(10):2775-2784.
88. Binder BY, Williams PA, Silva EA, Leach JK. Lysophosphatidic Acid and Sphingosine-1-Phosphate: A Concise Review of Biological Function and Applications for Tissue Engineering. Tissue Eng Part B Rev. 2015;21(6):531-542.
89. Hinsenkamp A, Kun K, Gajnut F, Majer A, Lacza Z, Hornyák I. Cell Attachment Capacity and Compounds of Fibrin Membranes Isolated from Fresh Frozen Plasma and Cryoprecipitate. Membranes (Basel). 2021;11(10).
90. Urist MR, Mikulski A, Boyd SD. A chemosterilized antigen-extracted autodigested alloimplant for bone banks. Arch Surg. 1975;110(4):416-428.
91. Majer A, Pesthy J, Besztercei B, Hinsenkamp A, Smeller L, Lacza Z, Benyó Z, Ruisanchez É, Hornyák I. Characterization of Native and Human Serum Albumin-Bound Lysophosphatidic Acid Species and Their Effect on the Viability of Mesenchymal Stem Cells In Vitro. Applied Sciences. 2022;12(16):8183.
92. Burnouf T. An overview of plasma fractionation. Annals of Blood. 2018;3.
93. Vácz G, Major B, Gaál D, Petrik L, Horváthy DB, Han W, Holczer T, Simon M, Muir JM, Hornyák I, Lacza Z. Hyperacute serum has markedly better regenerative efficacy than platelet-rich plasma in a human bone oxygen-glucose deprivation model. Regen Med. 2018;13(5):531-543.
94. Jurk K, Shiravand Y. Platelet Phenotyping and Function Testing in Thrombocytopenia. Journal of Clinical Medicine. 2021;10(5):1114.
95. Balbaied T, Moore E. Overview of Optical and Electrochemical Alkaline Phosphatase (ALP) Biosensors: Recent Approaches in Cells Culture Techniques. Biosensors. 2019;9(3):102.
96. Vimalraj S. Alkaline phosphatase: Structure, expression and its function in bone mineralization. Gene. 2020;754:144855.

97. Hsin IC, Yiwei W. Cell Responses to Surface and Architecture of Tissue Engineering Scaffolds. In: Daniel E, editor. Regenerative Medicine and Tissue Engineering. Rijeka: IntechOpen; 2011. p. Ch. 27.
98. Estrela-Lopis I, Brezesinski G, Möhwald H. Dipalmitoyl-phosphatidylcholine/phospholipase D interactions investigated with polarization-modulated infrared reflection absorption spectroscopy. Biophys J. 2001;80(2):749-754.
99. Villé H, Maes G, De Schrijver R, Spincemaille G, Rombouts G, Geers R. Determination of phospholipid content of intramuscular fat by Fourier Transform Infrared spectroscopy. Meat Science. 1995;41(3):283-291.
100. Movasaghi Z, Rehman S, ur Rehman DI. Fourier Transform Infrared (FTIR) Spectroscopy of Biological Tissues. Applied Spectroscopy Reviews. 2008;43(2):134-179.
101. Nzai JM, Proctor A. Determination of phospholipids in vegetable oil by fourier transform infrared spectroscopy. Journal of the American Oil Chemists' Society. 1998;75(10):1281-1289.
102. Alhazmi HA. FT-IR Spectroscopy for the Identification of Binding Sites and Measurements of the Binding Interactions of Important Metal Ions with Bovine Serum Albumin. Scientia Pharmaceutica. 2019;87(1):5.
103. Hinsenkamp A, Ézsiás B, Pál É, Hricisák L, Fülöp Á, Besztercei B, Somkuti J, Smeller L, Pinke B, Kardos D, Simon M, Lacza Z, Hornyák I. Crosslinked Hyaluronic Acid Gels with Blood-Derived Protein Components for Soft Tissue Regeneration. Tissue Eng Part A. 2021;27(11-12):806-820.
104. Baehrecke EH. Autophagy: dual roles in life and death? Nature Reviews Molecular Cell Biology. 2005;6(6):505-510.
105. Bandoh K, Aoki J, Taira A, Tsujimoto M, Arai H, Inoue K. Lysophosphatidic acid (LPA) receptors of the EDG family are differentially activated by LPA species. Structure-activity relationship of cloned LPA receptors. FEBS Lett. 2000;478(1-2):159-165.
106. Kim EK, Yun SJ, Do KH, Kim MS, Cho M, Suh D-S, Kim CD, Kim JH, Birnbaum MJ, Bae SS. Lysophosphatidic acid induces cell migration through the selective activation of Akt1. Experimental & Molecular Medicine. 2008;40(4):445-452.

107. Jans R, Mottram L, Johnson DL, Brown AM, Sikkink S, Ross K, Reynolds NJ. Lysophosphatidic acid promotes cell migration through STIM1- and Orai1-mediated Ca2+(i) mobilization and NFAT2 activation. J Invest Dermatol. 2013;133(3):793-802.
108. Song HY, Lee MJ, Kim MY, Kim KH, Lee IH, Shin SH, Lee JS, Kim JH. Lysophosphatidic acid mediates migration of human mesenchymal stem cells stimulated by synovial fluid of patients with rheumatoid arthritis. Biochim Biophys Acta. 2010;1801(1):23-30.
109. Li Z, Wei H, Liu X, Hu S, Cong X, Chen X. LPA rescues ER stress-associated apoptosis in hypoxia and serum deprivation-stimulated mesenchymal stem cells. J Cell Biochem. 2010;111(4):811-820.

9. Bibliography of the candidate's publications

Publications related to the dissertation

Majer A, Pesthy J, Besztercei B, Hinsenkamp A, Smeller L, Lacza Z, Benyó Z, Ruisanchez É., Hornyák I. Characterization of Native and Human Serum Albumin-Bound Lysophosphatidic Acid Species and Their Effect on the Viability of Mesenchymal Stem Cells In Vitro. Applied Sciences. 2022;12(16):8183. **IF: 2.7**

Hinsenkamp A, Kun K, Gajnut F, **Majer A**, Lacza Z, Hornyák I. Cell Attachment Capacity and Compounds of Fibrin Membranes Isolated from Fresh Frozen Plasma and Cryoprecipitate. Membranes (Basel). 2021;11(10). **IF: 4.2**

Other publications

Hinsenkamp A, Fülöp Á, Hricisák L, Pál É, Kun K, **Majer A**, Varga V, Lacza Z, Hornyák I. Application of Injectable, Crosslinked, Fibrin-Containing Hyaluronic Acid Scaffolds for In Vivo Remodeling. J Funct Biomater. 2022;13(3). **IF: 4.8**

Janovicz A, **Majer A**, Kosztelnik M, Geiszt M, Chun J, Ishii S, Tigyi G, Benyó Z, Ruisanchez É. Autotaxin-Lysophosphatidic Acid Receptor 5 Axis Evokes Endothelial Dysfunction via Reactive Oxygen Species Signaling. Experimental Biology and Medicine. 2023; **IF: 3.2**

Cumulative impact factor of the candidate's publications: **15.262**

10. Acknowledgements

I am very grateful to my supervisor, Éva Ruisanchez for her support and guidance. I would like to thank her for always making time for me during my undergraduate research work and the four years of my PhD studies and helping my research with her advices.

I also would like to thank to my co-supervisor, István Hornyák for his encouragement and advices. I am grateful for his professional ideas and help during the experiments, and publications.

I am very thankful to Adél Hinsenkamp, my colleague and friend, for not only teaching me the research techniques, but that I could always count on her in everything.

I would like to thank to Zsombor Lacza and OrthoSera Medical Zrt. for their cooperation and the support of my research.

I am thankful to Professor Zoltán Benyó for providing the place and infrastructure for my research at the Institute of Translational Medicine and for his encouragement ever since I was a student researcher in his lab.

In addition, I am very grateful to Dániel Veres for thoroughly reviewing my thesis. His comments and suggestions have greatly improved the quality of this thesis.

I am very grateful to my official reviewers, Tímea Feller, and Krisztina Ella for thoroughly, and critically reviewing my thesis.

I would like to express my sincere gratitude to all my co-authors for their effort, and all former and current colleagues at the Institute of Translational Medicine for their support.

Finally, I am very grateful to my husband, and to my whole family. Without their encouragement and support this thesis could not have been accomplished.